

26



Holocene land cover change in North America: continental

- trends, regional drivers, and implications for vegetationatmosphere feedbacks
- Andria Dawson*†¹, John W. Williams†², Marie-José Gaillard³, Simon J Goring², Behnaz
- 6 Pirzamanbein⁴, Johan Lindstrom⁵, R. Scott Anderson⁶, Andrea Brunelle⁷, David Foster⁸, Konrad Gajewski⁹, Daniel G. Gavin¹⁰, Terri Lacourse¹¹, Thomas A Minckley¹², Wyatt Oswald¹³, Bryan
- 8 Shuman¹², Cathy Whitlock¹⁴
- 10 Department of Mathematics and Computing, Department of Biology, Mount Royal University, Calgary, AB T3F6K6
- 12 ²Department of Geography and Center for Climatic Research, University of Wisconsin-Madison, Madison, WI 53706
- 3Department of Biology and Environmental Science, Linnaeus University, SE 39231 Kalmar, Sweden
 4Department of Statistics, School of Economics and Management, Lund University, SE-220 07 Lund, Sweden
- 5 Division of Mathematical Statistics, Centre for Mathematical Sciences, Lund University, SE-221 00 Lund, Sweden
 6 School of Earth and Sustainability, Northern Arizona University, Flagstaff, AZ 86011
- 7Geography Department, University of Utah, Salt Lake City, UT 84112
 8Harvard Forest, Harvard University, Petersham, MA 01366
- ⁹Département de Géographie, Environnement et Géomatique, Université d'Ottawa, Ottawa, ON K1N 6N50
 ¹⁰Department of Geography, University of Oregon, Eugene, OR 97403
- 22 ¹¹Department of Biology and Centre for Forest Biology, University of Victoria, Victoria, BC V8P 5C2 ¹²Department of Geology and Geophysics, University of Wyoming, Laramie, WY 82071
- 24 ¹³Marlboro Institute for Liberal Arts and Interdisciplinary Studies, Emerson College, Boston, MA 02116 and ¹⁴Department of Earth Sciences, Montana State University, Bozeman, MT 59717
 - *Correspondence email: adawson@mtroyal.ca
- †These authors contributed equally to the development of this manuscript





30 Abstract

Land cover governs the biogeophysical and biogeochemical feedbacks between the land surface and 32 atmosphere. Holocene vegetation-atmosphere interactions are of particular interest, both to understand the climate effects of intensifying human land use and as a possible explanation for the Holocene 34 Conundrum, a widely studied mismatch between simulated and reconstructed temperatures. Progress has been limited by a lack of data-constrained, quantified, and consistently produced reconstructions of 36 Holocene land cover change. As a contribution to the Past Global Changes (PAGES) LandCover6k Working Group, we present a new suite of land cover reconstructions with uncertainty for North America, 38 based on a network of 1445 sedimentary pollen records and the REVEALS pollen-vegetation model coupled with a Bayesian spatial model. These spatially comprehensive land cover maps are then used to 40 determine the pattern and magnitude of North American land cover changes at continental to regional scales. Early Holocene afforestation in North America was driven by rising temperatures and deglaciation, and this afforestation likely amplified early Holocene warming via the albedo effect. A 42 continental-scale mid-Holocene peak in summergreen trees and shrubs (8.5 to 4 ka) is hypothesized to 44 represent a positive and understudied feedback loop among insolation, temperature, and phenology seasonality. A last-millennium decrease in summergreen trees and shrubs with corresponding increases in 46 open land likely was driven by a spatially varying combination of intensifying land use and neoglacial cooling. Land cover trends vary within and across regions, due to individualistic taxon-level responses to 48 environmental change. Major species-level events, such as the mid-Holocene decline of eastern hemlock, may have altered regional climates. The substantial land-cover changes reconstructed here support the 50 importance of biogeophysical vegetation feedbacks to Holocene climate dynamics. However, recent model experiments that invoke vegetation feedbacks to explain the Holocene Conundrum may have 52 overestimated the land cover forcing by replacing Northern Hemisphere grasslands >30°N with forests; an ecosystem state that is not supported by these land cover reconstructions. These Holocene 54 reconstructions for North America, along with similar LandCover6k products now available for other continents, serve the Earth system modeling community by providing better-constrained land cover 56 scenarios and benchmarks for model evaluation, ultimately making it possible to better understand the regional- to global-scale processes driving Holocene land cover dynamics.

58





1. Introduction

60 Vegetation is the great mediator of biogeophysical and biogeochemical interactions between the land surface and the atmosphere (Bonan and Doney, 2018; Harrison et al., 2020; Pongratz et al., 2010; Gaillard 62 et al., 2010). Enhanced carbon uptake and sequestration by terrestrial ecosystems is an essential component to contemporary negative-net CO₂ emission scenarios needed to stabilize the climate system 64 and mitigate the dangerous impacts already emerging (Rogelj et al., 2018; van Vuuren et al., 2017). During the Holocene, as cryosphere-ocean-atmosphere feedbacks waned and anthropogenic land use intensified (Ruddiman, 2013; Stephens et al., 2019), vegetation-atmosphere feedbacks and forcings 66 increased in importance, particularly in regions where climate variability interacted with major changes in 68 vegetation structure. Examples include soil and vegetation feedbacks that amplified precessional-driven variations in monsoonal rainfall intensity in North Africa and Asia (Chen et al., 2021; Chandan and 70 Peltier, 2020), and increases in high-latitude tree cover, which decreased wintertime albedo and increased temperatures (Williams et al., 2011; TEMPO (Testing Earth System Models with Paleo-Observations), 72 1996; Foley et al., 1994). Intensified human land use and resulting greenhouse gas emissions may have delayed Northern Hemisphere late-Holocene cooling and glaciation (Ruddiman, 2003). However, initial 74 models of global anthropogenic land cover change (ALCC) (Kaplan et al., 2009; Klein Goldewijk et al., 2011, 2010) over the Holocene were largely unconstrained by paleoecological and archaeological observations and so differed widely in their estimated size and scope of the anthropogenic footprint. More 76 recently, Holocene increases in vegetation cover have been invoked to explain the Holocene Temperature 78 Conundrum, a discrepancy between proxy and model-estimated temperature during the early- to mid-Holocene (Thompson et al., 2022; Kaufman and Broadman, 2023), but global simulations of vegetation-80 climate feedbacks during the Holocene are not constrained by observational data. At subcontinental scales, data-constrained studies of Holocene climate-vegetation feedbacks in Europe indicate that mid-82 Holocene vegetation changes relative to pre-Industrial baselines could have warmed winters in some areas by 4-6°C in northeastern Europe (Strandberg et al., 2022a, 2014). 84 Hence, there is an on-going need for comprehensive and accurate proxy-based reconstructions of past land cover at regional to global extents (Gaillard and Group, 2015; Gaillard et al., 2018, 2010). These 86 reconstructions can then be used with Earth system models (ESMs) to test hypotheses about the physical, biological, and anthropogenic processes that drove Holocene climate variability (Harrison et al., 2020). Fossil pollen records offer the primary observational constraint on past vegetation composition and 88 structure, with thousands of records now available globally. Efforts to systematically map late-Quaternary 90 land cover using fossil pollen data and well-defined rulesets began in the late 1990s with the Biome6000 project (Prentice et al., 2000, 2011). Since then, the continental-scale pollen databases launched in the





Neotoma Paleoecology Database (Neotoma), an international, multi-proxy, curated data resource that 94 helps tame issues of data heterogeneity through community curation by experts (Williams et al., 2018). Neotoma thus enables global-scale analyses of past vegetation and climate change (e.g. Mottl et al., 2021; 96 Herzschuh et al., 2023). Multiple pollen-vegetation models (PVMs) have been developed to make quantitative inferences 98 about past vegetation. Some PVMs involve relatively simple but effective transfer functions, such as the modern analogue technique (Williams et al., 2011) or rule-based systems for classifying land cover 100 (Prentice et al., 2000; Cruz-Silva et al., 2022; Fyfe et al., 2010). Others are process-based proxy system models (Evans et al., 2013) that attempt to represent the processes governing the atmospheric transport 102 and deposition of pollen, such as the REVEALS and LOVE (Sugita, 2007a, c) or STEPPS (Dawson et al., 2019a). Efforts continue to test and refine the parameterizations of these models through paired analyses 104 of pollen assemblages and forest composition at local to landscape scales (Liu et al., 2022). In response to these scientific needs and opportunities, the Past Global Changes (PAGES) 106 LandCover6k working group was launched as an international effort (Gaillard and Group, 2015) to reconstruct vegetation globally for the Holocene. LandCover6k, led by experts typically working at 108 continental scales, has had the explicit aim of creating vegetation reconstructions that can better constrain past histories of anthropogenic land use in ESMs and is mostly based on networks of fossil pollen 110 records. To facilitate the use of these vegetation reconstructions in ESMs, the REVEALS PVM has been used for all LandCover6k reconstructions, with standard model parameterizations and standard protocols 112 for pollen data handling. LandCover6k gridded REVEALS reconstructions at the continental scale have been published so far for Europe (Githumbi et al., 2022a, b; Trondman et al., 2015; Serge et al., 2023) and 114 China (Li et al., 2023b). However, no comparable REVEALS-based land cover reconstructions are available for North America, despite a comparable density of fossil pollen records to these other regions 116 (Stegner and Spanbauer, 2023) and prior regional-scale applications of REVEALS in North America (Sugita et al., 2010; Chaput and Gajewski, 2018). 118 REVEALS uses pollen counts, pollen productivity estimates, pollen fall speeds, atmospheric conditions, and sedimentary basin type and size to estimate vegetation composition for a given time 120 period. REVEALS accounts for the processes of differential pollen production (determined by pollen productivity estimates) and dispersal-deposition (determined by the pollen fall speeds, atmospheric 122 conditions, and sedimentary basin type and size). While REVEALS reconstructions usually combine information from multiple pollen records, REVEALS 124 is not explicitly spatial, and so does not support the interpolation of inferences to places with no pollen records. To address this issue, other researchers have developed a statistical approach to spatially

1980s and 1990s (Grimm et al., 2013) have coalesced along with other paleoecological data into the





126 interpolate REVEALS-based land cover estimates from individual grid cells to all cells within the grid, including estimates of uncertainty (Pirzamanbein et al., 2014, 2018a). The approach uses a Bayesian 128 hierarchical model with spatial dependence specified according to a Gaussian Markov Random Field (GMRF; (Lindgren et al., 2011); we refer to the two-step process of REVEALS-based estimation 130 followed by this spatial interpolation as the REVEALS-GMRF approach. REVEALS-GMRF has been used to develop spatially continuous gridded vegetation reconstructions in Europe to assess vegetation-132 climate feedbacks resulting from natural and anthropogenic land cover change (Strandberg et al., 2022b) and to evaluate ALCC models (Kaplan et al., 2017) and dynamic vegetation models (Pirzamanbein et al., 134 2020; Dallmeyer et al., 2023; Zapolska et al., 2023). Here we adopt the REVEALS-GMRF approach to reconstruct land cover changes in North 136 America during the Holocene. This work relies on 1445 Holocene pollen records drawn from Neotoma and its constituent database, the North American Pollen Database (NAPD), with a targeted data-138 mobilization campaign employed to add more records to the NAPD for western North America. Using these data, we reconstruct the fractional cover of 32 plant taxa and three land cover types (LCTs): 140 evergreen trees and shrubs (ETS), summergreen trees and shrubs (STS), and open vegetation/land (OVL, including grasses, herbs, and low shrubs) from 12,000 years ago (12 ka) to present. We present the 142 Holocene vegetation reconstructions by working across scales, first describing continental-scale trends in land cover, then shifting to several regional-scale case studies to show how the continental-scale trends 144 emerge from taxon-level dynamics that vary within and among regions, with respect to key taxa, drivers, and resultant land-cover changes. We then zoom out to discuss the continental-scale drivers of Holocene 146 land cover change in North America and possible biophysical implications of these changes for Holocene vegetation-atmosphere interactions and the Holocene Conundrum. Lastly, we discuss the potential 148 limitations of the REVEALS-GMRF approach and the opportunities now available for well-constrained

2. Data and methods

150

2.1 Pollen data and data mobilization for western North America

hemispheric- to global-scale studies of vegetation-atmosphere interactions.

Western North America has traditionally been underrepresented in the NAPD and Neotoma, but the density of fossil pollen records in western North America has steadily increased in recent decades, as
 multiple teams have worked to collect new records, often focusing on interactions among past vegetation, fire, climate, and human dynamics (Anderson et al., 2008; Gavin and Brubaker, 2014; Marlon et al.,
 2012; Iglesias et al., 2018; Alt et al., 2018). Many of these datasets were contributed to Neotoma





(Williams et al., 2018) when originally published, while others were contributed to Neotoma for an opendata mobilization campaign conducted for this paper and PAGES LandCover6k (Gaillard et al., 2018).

After this effort, 1582 North American Holocene pollen records were downloaded from Neotoma 160 (Supp. Table 1). Each record included pollen count data at a series of depths. For methodological consistency (Flantua et al., 2023), we refit all age-depth models using a custom-built workflow 162 (https://github.com/andydawson/bulk-bchron that assessed chronological constraints and then used these chronological constraints and IntCal20NH (Reimer et al., 2020) to fit the Bchron age-depth model 164 (Parnell et al., 2008). This resulted in 1445 records with age-depth models. Ages of the youngest and oldest chronological constraints were used to determine the reliable age range for each record; we limited 166 extrapolation of pollen sample ages beyond the youngest or oldest constraints to 1000 years. Pollen types were aggregated to taxa using the taxa list in the North American Modern Pollen Database (Whitmore et 168 al., 2005). We used a subset of 32 taxa for this analysis, choosing the most abundant taxa, several openland indicators, and taxa with available estimates of relative pollen productivity (Tables 2, 5).

170

2.2 REVEALS (regional reconstructions)

172 Pollen-based land cover reconstructions were performed using the REVEALS pollen-vegetation model (Sugita, 2007b), and based on the standard protocol for PAGES LandCover6k (Trondman et al., 2015; 174 Githumbi et al., 2022a). This model estimates the relative abundance of plant taxa, along with the standard error of these estimates, given pollen counts and input parameters that represent sedimentary 176 basin size and type, pollen productivity estimates (PPEs), pollen fall speeds, and atmospheric conditions. REVEALS was developed to operate at the regional scale (Sugita, 2007a; Hellman et al., 2008a, b); 178 inferences of plant relative abundance represent the background vegetation over large areas (suggested as 100 km x 100 km in (Hellman et al., 2008b), but this scale is variable). REVEALS traditionally has been used to infer plant relative abundance from records from large lakes (>50 ha), but has been tested and 180 applied to regions with records from a number of smaller lakes. The REVEALS model accounts for both 182 differential productivity and dispersal among taxa. Differential productivity is determined by taxonspecific PPEs, while dispersal is modeled according to a Gaussian plume (Sutton, 1953) or Lagrangian 184 dispersal-deposition model (Kuparinen et al., 2007), both of which require the specification of atmospheric conditions including wind speed. REVEALS accounts for differential dispersibility among 186 taxa using pollen fall speeds. See (Sugita, 2007b; Githumbi et al., 2022a) for a more detailed and theoretical description of REVEALS. We implement REVEALS using the REVEALSinR R package 188 (Theuerkauf et al., 2016). REVEALS estimates for other regions included in the LandCover6k effort (Li et al., 2023a; Githumbi et al., 2022a) were developed using more traditional implementations of this



192

194

196

198

200

202

204

206

208

210

212

214

216

218

220

222



model (LRA.REVEALS.v6.2.4.exe (Sugita, unpublished) and LRA R package (Abraham et al., 2014)), which differ slightly in their calculation of the standard errors of relative abundances.

Pollen source areas and the relative representation of plant taxa in the REVEALS dispersaldeposition model are affected by sedimentary basin type (e.g. lake, mire) and area (Sugita, 2007a; Trondman et al., 2016). Basin type is typically included in Neotoma metadata for pollen datasets, but not all datasets include metadata on basin area. To determine basin area for these datasets, we developed a standard workflow (Goring, 2021); https://github.com/NeotomaDB/neotoma lakes). First, we used hydrological databases (National Hydrography Dataset (United States Geological Survey, 2022), National Hydro Network (Natural Resources Canada, 2022)) to assign basin areas to datasets whose coordinates fell within a water-body polygon. Second, for dataset coordinates that landed outside a water-body polygon, we used Google Earth Engine to identify the basin. These basins were traced using the polygon tool in Google Earth Engine, and basin area was calculated from polygon area. Not all basins could be identified, however, particularly for pre-GPS sites in Neotoma with imprecise coordinates. Third, for sites still without basin area, we assigned a size of 50 ha. In the context of the REVEALS model, this represents a medium-sized lake. This decision avoids the potential biases from assigning large or small lake areas, although site-level reconstructions may over- or under-represent taxa if basin area (and hence pollen source area) is inaccurate (Jackson, 1990; Davis, 2000; Liu et al., 2022). All basin areas recovered in the first and second steps were added as site-level metadata to Neotoma, along with dataset notes.

We used PPE and fall speed datasets from Wieczorek and Herzschuh (2020) for the Northern Hemisphere extra-tropics. Specifically, we used the North America continental-scale datasets, which include PPE (with grass as the reference taxon) and fall speed values for 30 of the 32 taxa we consider in this work. For *Ambrosia* (ragweed) and *Tsuga* (hemlock), which were not included in Wieczorek and Herzschuh (2020), we use PPE and fall speed values from a previously compiled North America dataset (Dawson et al., 2016; Trachsel et al., 2020). Additionally, for the *Larix* (larch) fall speed, we used the value for *Larix laricina* from (Niklas, 1984), which is the dominant species in eastern and northern North America. This estimate is an order of magnitude smaller than the *Larix* taxon-level fall-speed estimate included in (Wieczorek and Herzschuh, 2020), which originates from (Bodmer, 1922)). We experimented with fall-speed datasets that included these larger *Larix* fall-speed estimates; these vegetation reconstructions indisputably overrepresented larch.

We used the Gaussian plume dispersal model with a wind speed of 3 m/s and neutral atmospheric conditions (vertical diffusion coefficient cz=0.12; turbulence parameter n=0.25; wind speed u=3 m/s; see (Jackson and Lyford, 1999a)), to be consistent with the dispersal model specified in the LandCover6k protocol for Northern Hemisphere reconstructions (Dawson et al., 2018; Githumbi et al., 2022a). We set



244

246

248

250

252

254



the region cutoff to the REVEALSinR function default of 100 km; this specifies the maximum distance that most pollen will originate from (Sugita, 2007a; Theuerkauf et al., 2016).

We reconstructed land cover for 25 time intervals that cover the Holocene. These time intervals 226 were defined according to the LandCover6k working group protocol (Trondman et al., 2015) (SI Table 4). Time intervals are specified in kiloyears before present (ka), where present is defined as 1950 CE, but 228 for time intervals <1ka we also note the Common Era (CE) timescale. Intervals in the period from 11.7 to 0.7 ka have a 500-year temporal grain (11.7 to 11.2 ka; 11.2 to 10.7 ka; etc.), while the three most recent intervals have a finer temporal grain (0.7-0.35 ka [1250-1600 CE]: 350 years; 0.35-0.1 ka [1600-1850 230 CE]: 250 years; 0.1-(-0.074) ka: 174 years [1850-2024 CE]) in order to better capture the changes 232 associated with intensifying anthropogenic land use over the last five centuries. Pollen samples were assigned to a time interval based on their mean calibrated radiocarbon age. If multiple samples for a 234 record fell within the same interval, pollen counts were summed by taxon, so that each record would have at most one set of pollen counts per time interval. We used a grid resolution of 1°x1°, also as specified by 236 the LandCover6k protocol. Within a grid cell, REVEALS reconstructions for multiple sites were averaged, as is standard practice (Sugita, 2007a). Taxon-level reconstructions were aggregated to three 238 land cover categories (SI Table 5): summergreen trees and shrubs (STS), evergreen trees and shrubs (ETS), and open vegetation/land (OVL), which includes grasses, herbs, and low-stature shrubs. All trees 240 and shrubs (ATS) is calculated as the sum of STS and ETS.

242 2.3 REVEALS-GMRF (spatial modeling and interpolation with uncertainty)

Here, we use the REVEALS-GMRF Bayesian hierarchical model (Pirzamanbein et al., 2018b) to spatially interpolate the REVEALS-based land cover reconstructions. REVEALS-GMRF exploits the spatial dependence in land cover using a Gaussian Markov Random Field, and permits the characterization of uncertainty given the empirical land cover product. As in Pirzamanbein et al. (2018), we use elevation as a covariate. Although including simulations of land cover as an additional covariate can further improve the reliability of resulting land cover maps (Pirzamanbein et al., 2020), the intent of our work is to develop a spatial land cover product suitable for validation of and assimilation with dynamic vegetation, land use, and Earth System models. Hence, to maintain independence, we refrain from using simulated land cover as a covariate. To quantify overall uncertainty of a grid cell for a specified time period, we computed the area of confidence regions (CR; (Pirzamanbein et al., 2018a)). Smaller CR values indicate higher confidence, while larger CR values indicate more uncertainty. As in Pirzamanbein et al. (2018), a CR threshold is determined using the complete set of CR values. Accordingly, any grid cells with a CR greater than a threshold of 9 were omitted from spatial reconstructions (Githumbi et al., 2022c). The





result of this spatial interpolation is a set of empirically-based land cover maps for North America and the LandCover6k time intervals, with uncertainty.

258

274

276

278

280

282

2.4 Calculation of proportional changes and mapped anomalies

260 To summarize continental-scale land-cover dynamics through time, we built time series of both mean relative cover and area-weighted relative cover. We used recently updated ice sheet maps (Dalton et al., 262 2020) to identify glaciated and unglaciated grid cells for each time period, then calculated the fraction of unglaciated land cover for each time period. We then calculated the mean relative cover of each land 264 cover type for each time period, across all unglaciated grid cells at that time period. Mean relative cover usefully summarizes land cover change within ice-free regions, but does not track the overall increases in 266 vegetated land area in North America during the last deglaciation. To calculate area-weighted relative cover, for each time period, we multiplied the relative cover of each grid cell by the cell area, and then 268 summed the relative cover of each land cover type across space for unglaciated land grid cells. We then divided these summed area-weighted cover values for each time period by the sum of total unglaciated 270 land area at 0.25 ka. Because the number of unglaciated land grid cells changes through time, while the denominator is constant, this area-weighted metric of relative cover is affected by both available land and 272 changes in land cover proportion, resulting in a proportional metric that is sensitive to continental-scale increases in vegetation cover.

For each pair of time intervals, we calculated land cover change as grid-cell scale differences for each of the three land cover classes. After visually identifying areas of large land cover changes (Supp. Fig. 3), we identified several regions for further investigation: the northeastern US and southeastern Canada (NEUS/SEC), eastern Canada (ECAN), western Canada and Alaska (WCAN/AK), and the Pacific Coast, Cascades, and Sierra Nevada (PCCS) based on areas of greatest change and pollen-site density. We then assessed vegetation change for each region at both the taxon and land cover scales, using the REVEALS grid-cell estimates of taxon mean abundances and the REVEALS-GMRF interpolated estimates of mean cover for the land cover types.

3. Results

3.1 Data coverage

The assembled dataset of 1445 fossil pollen records has good coverage across the continental US and Canada (Fig. 1a). Areas of relatively high site density include the Great Lakes region of the US and
 Canada, the northeastern US, the Rocky Mountains, the Pacific Coast, and central Alaska. Given good data-mobilization efforts for the US and Canada, this distribution reasonably approximates the true

https://doi.org/10.5194/cp-2024-6 Preprint. Discussion started: 20 February 2024 © Author(s) 2024. CC BY 4.0 License.





distribution of fossil pollen records, so spatial gaps usually represent lack of available sites (e.g. few lakes or wetlands in arid regions) or inaccessibility (e.g. high Arctic). Conversely, a lower site density in
Mexico and Central America is partially due to less extensive open-data mobilization efforts in these regions. Temporally, the distribution of oldest samples (an indicator of record length) is smooth (Fig. 1b), with rapid accumulation of sites between 11.7 and 11 ka (33% of sites have an oldest sample in this interval) and between 0.5 and -0.074 ka (74% of sites have a youngest sample in this interval).

10





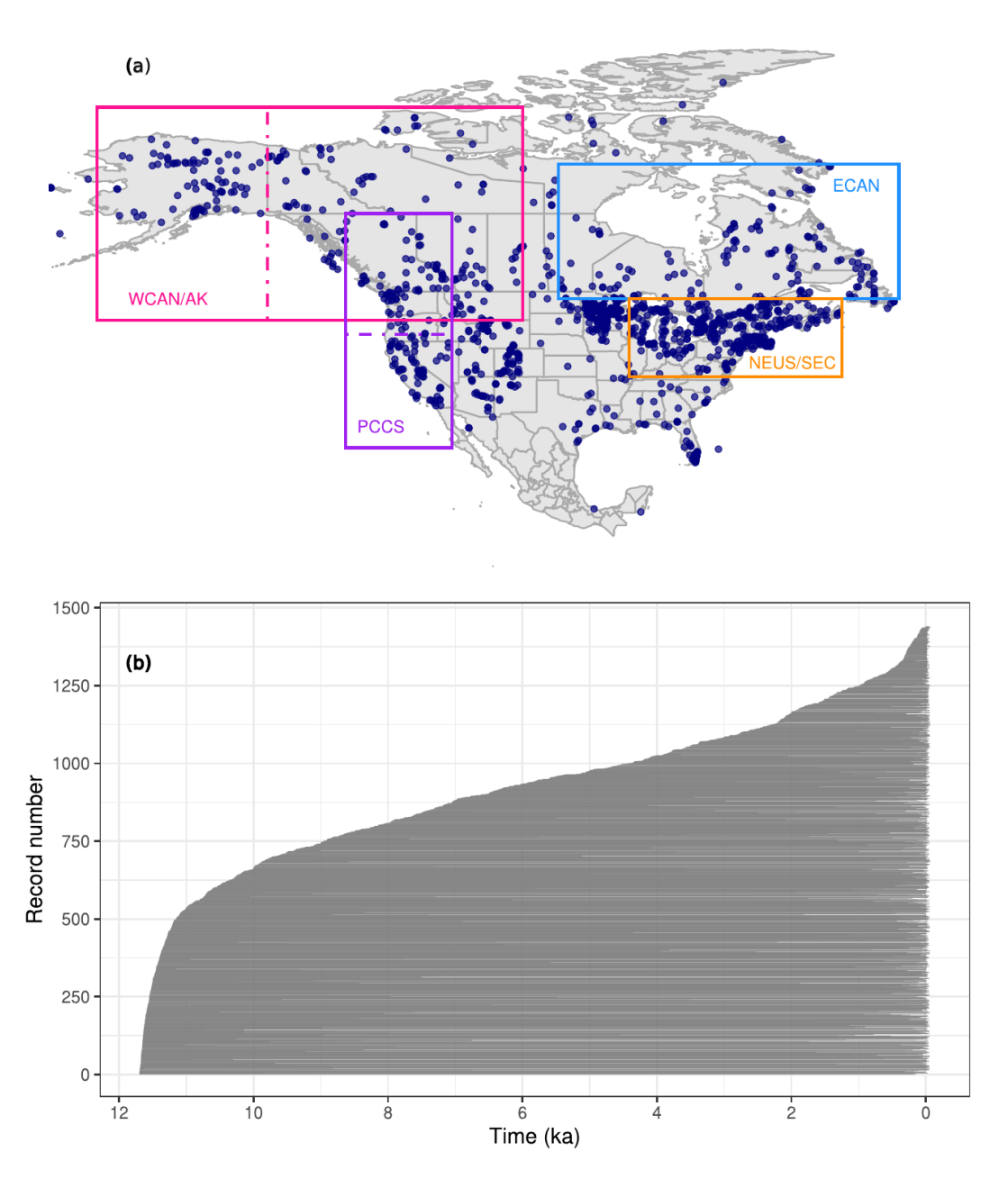


Figure 1: The spatiotemporal distribution of fossil pollen data used here. A) Map indicating the spatial distribution of sites recovered from the Neotoma Paleoecology Database, as well as the case study regions
 (WCAN/AK: Western Canada and Alaska; PCCS: Pacific Coast, Cascades, and Sierra Nevada; ECAN: Eastern Canada; and NEUS/SEC: North-Eastern US and South-Eastern Canada). B) Temporal extent of



308



all sites, in which each site is represented by a horizontal gray line between the site's oldest and youngest
 Holocene samples. Sites are ordered by age of the oldest sample, reported as ka. Samples older than 11.7
 ka are not shown.

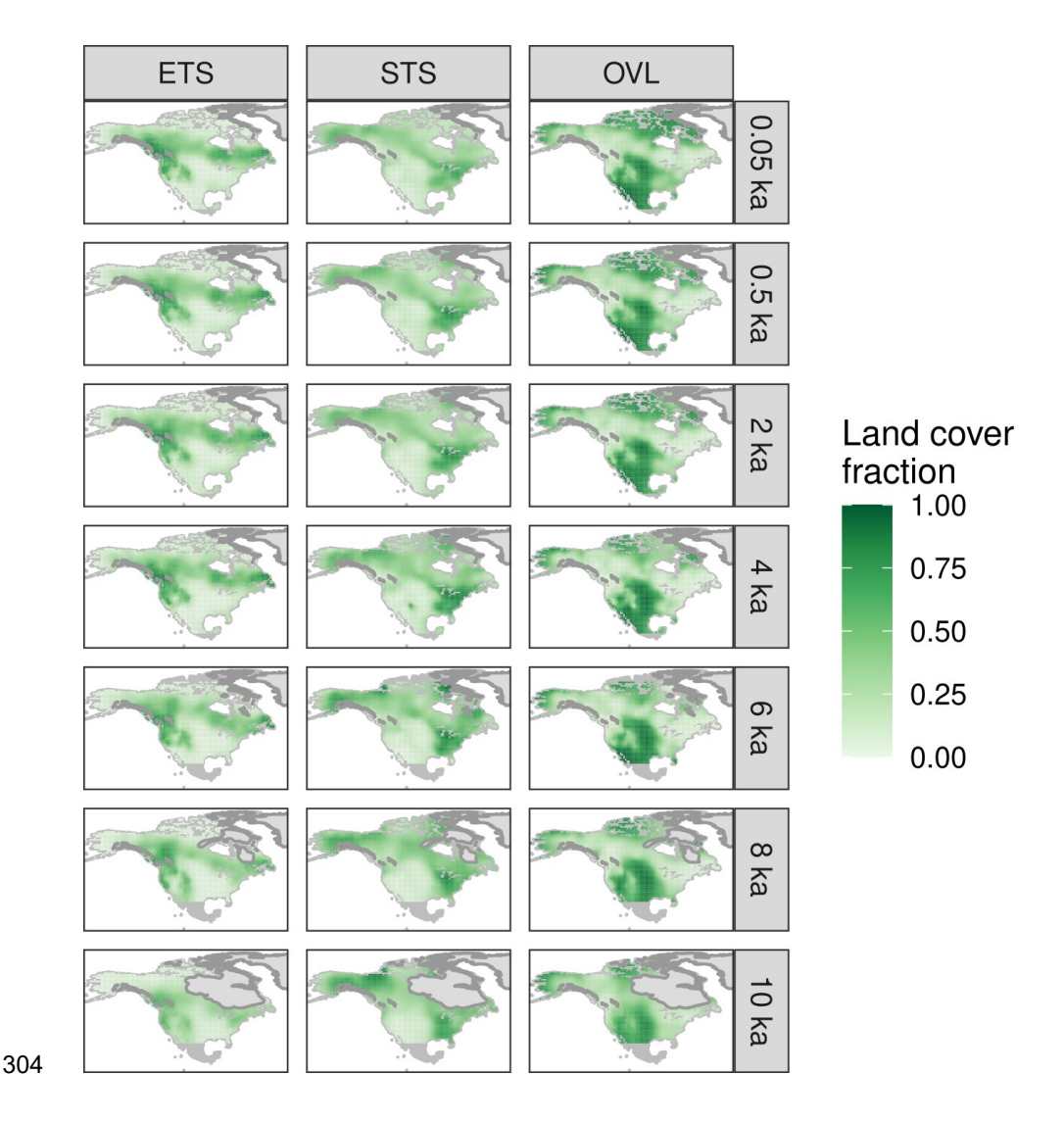


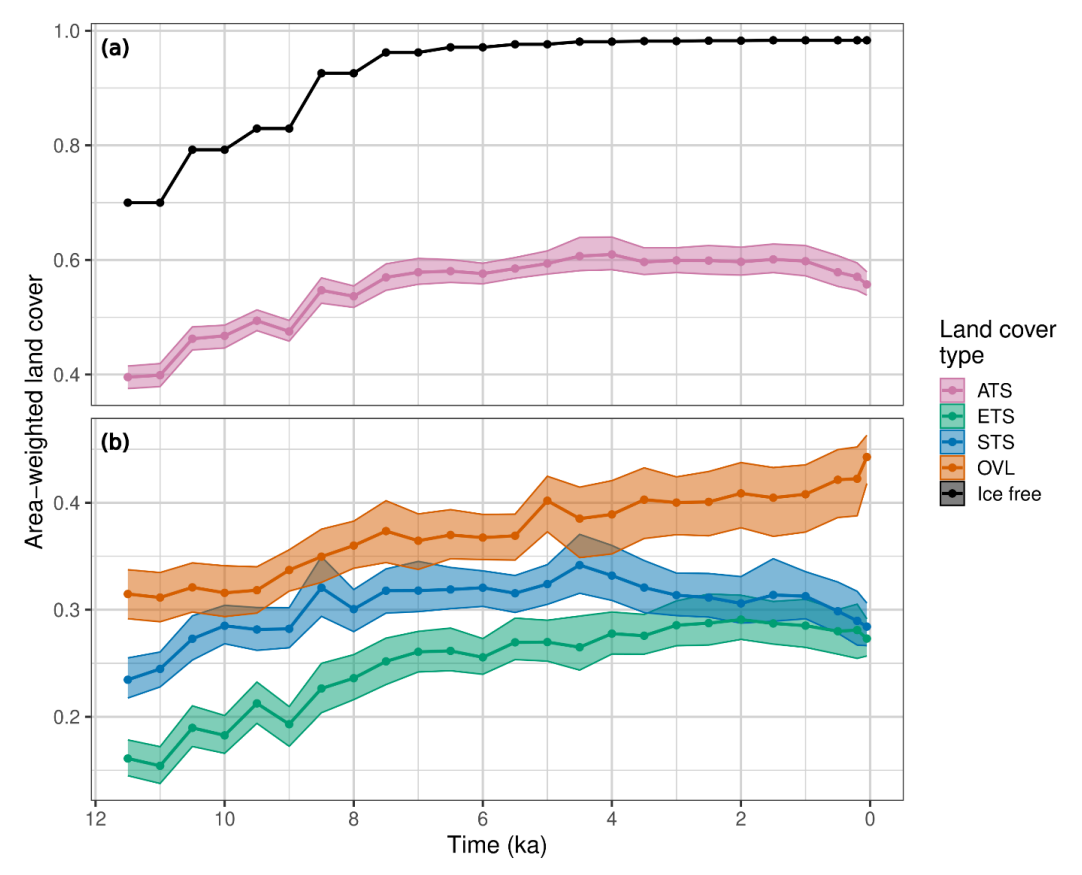
Figure 2: Interpolated REVEALS-based estimates of fractional cover for evergreen trees and shrubs (ETS), summergreen trees and shrubs (STS), and open land (OVL). Laurentide and Cordilleran Ice Sheet extents (Dalton et al., 2020) are indicated by gray polygons Estimates are presented on a 1°x1° grid, for selected time periods, with ages reported as ka. Map ordering follows the geological convention of oldest





maps at bottom. The spatial domain for interpolation includes all unglaciated locations in North America between 17 and 79°N.

312



314

316

318

320

Figure 3: (a) Holocene trends in area-weighted cover of all trees and shrubs (ATS) in North America (pink curve with 95% uncertainty envelope), expressed relative to present unglaciated land area (see Methods), and the fraction of unglaciated land relative to continental land area (black). Total cover is the sum of the evergreen and summergreen trees and shrubs. (b) Trends in the area-weighted cover of evergreen (ETS), summergreen (STS) and open vegetation/land (OVL) for North America. For both plots, land cover estimates are based on the interpolated data for the spatial domain shown in Fig. 2.

322

3.2 Continental-scale trends in Holocene land cover





during the Holocene (Fig. 2). Persistent features include belts of high evergreen tree cover in the 326 mountainous West and Canada, high summergreen tree cover in the eastern US, moderate to high cover of summergreen trees and shrubs in Alaska and northern Canada, and high proportions of open vegetation in 328 the Great Plains, western Alaska, and Arctic Canada (Fig. 2). However, despite this broadly stable spatial configuration, there were large continental-scale 330 changes in the area-weighted fractional cover of land cover types in North America during the Holocene, particularly during the early Holocene (Fig. 3a, Supp. Fig. S3). From 11.7 to 7 ka, the area-weighted 332 fraction of forested land cover increased from about 56 to 91%. This increase closely tracked the increase in available land surface area, as the Laurentide Ice Sheet retreated (Fig. 3a) (Dalton et al., 2020). 334 During the early Holocene, the largest gains in forest cover were across deglaciated western Canada and ice-marginal areas in eastern Canada (Fig. 2, Supp. Fig. S3). Forest cover continued to expand between 336 7.5 and 4.5 ka (Fig. 3a), even though the Laurentide Ice Sheet had disappeared by ~6 ka, with the largest afforestation in the northern Great Plains of central Canada and in recently deglaciated regions of eastern Canada (Fig. 2, Supp. Fig. S3). Continental-scale forest cover remained stable from 4.5 to 1.5 ka, then 338 declined after 1.5 ka (Fig. 3a). The late-Holocene decline in forest cover was most pronounced in the 340 eastern US and in Arctic and boreal Canada where open vegetation began increasing after 4 ka (Fig. 2, Supp. Fig. S3, S4). 342 Within these Holocene trends, the three land cover types followed differing trajectories (Fig. 3b). All three show a strong increase between 11.7 and 7.5 ka in their area-weighted relative cover, again 344 tracking ice retreat. After 7.5 ka, however, the three trajectories diverged. Evergreen trees and shrubs continued to rise slowly but steadily from 7.5 to 2 ka, then declined slightly (Fig. 3b). Summergreen trees 346 and shrubs reached peak area-weighted cover at 4.5 ka, then declined, with an accelerated decline after 1.5 ka. The proportion of open lands remained largely stable from 7.5 to 4.5 ka, then increased, with an 348 accelerating increase after 2 ka. A close examination of the continental-scale anomaly maps (Supp. Figs.

S3, S4) suggests a fairly complex spatial mosaic for each land cover type, with the continental-scale

trends emerging from a welter of regional-scale phenomena. For example, widespread gains in evergreen trees and shrubs across much of Canada and Alaska between 6 and 4 ka were partially offset by large

losses in the eastern US and southeastern Canada over the same period (Supp Fig. S3). Because different plant species predominate in different regions of North America, these continental-scale trends in land

cover were the emergent outcomes of individualistic species-level responses to changing climates and, in

some places, intensifying land use (Williams et al., 2004).

At a continental scale, the spatial configuration of land cover in North America has been broadly stable

356

350

352

354



374

376

378

380

382

384

386

388

390



3.3 Regional case studies

3.3.1 Northeastern US & Southeastern Canada (NEUS/SEC)

360 For the mostly forested NEUS/SEC, after initial afforestation and loss of open lands during the early Holocene (10 to 8 ka), the central dynamic has been shifts in the relative cover of evergreen and 362 summergreen trees and shrubs (Fig. 4a, Supp. Fig. S5). The fractional cover of evergreen trees and shrubs declined throughout the early to middle Holocene (10 to 4 ka) in the southern part of the domain, which 364 intensified to widespread loss across the NEUS/SEC (6 to 4 ka), but then reversed after 4 ka, with recovery and regrowth of evergreen trees and shrubs (Fig. 4a). The western increase in open lands 366 between 8 and 4 ka is caused by the eastward expansion of prairie due to drier conditions (Williams et al., 2009b), while the decrease in open lands from 4 to 0.5 ka is due to increased moisture availability that 368 resulted in a westward shift of the prairie-forest border and increase in summergreen forest taxa in the eastern Midwest (Umbanhowar et al., 2006). Overall, the low proportions of open vegetation in the 370 NEUS/SEC from 9 ka until European settlement (Fig. 4B) likely represents these western prairies and local wetlands, which expanded in the late Holocene in parts of the NEUS/SEC (Brugam and Swain, 372 2000; Ireland and Booth, 2010), rather than grasslands or other open lands in eastern deciduous forests (Faison et al., 2006).

At a taxon level, most changes in evergreen cover can be attributed to regional declines of cold-tolerant conifers such as *Picea glauca*, *P. mariana*, and *P. rubens* (white, black, and red spruce); *Pinus banksiana*, *P. resinosa*, and *P. strobus* (jack, red, and white pine), and *Abies balsamea* (balsam fir) between 10 and 6 ka (Fig. 4c, Supp. Fig. S6) (Spear et al., 1994; Jackson and Whitehead, 1991; Jackson et al., 1997). These changes, combined with the zonal pattern of evergreen expansion in the northern NEUS/SEC and declines in the southern part, suggest that much of the evergreen tree and shrub cover changes during the early to middle Holocene can be attributed to postglacial northward shifts in tree distributions in response to rising temperatures and deglaciation.

A second major feature is the well-known and dramatic expansion, collapse, and re-expansion of *Tsuga canadensis* (eastern hemlock), a cool-temperate conifer that typically occupies warmer climates than *Abies balsamea* (Thompson et al., 1999). Investigations continue into understanding the abrupt and widespread collapse in *Tsuga canadensis*, which differed from the overall evergreen trend. The collapse occurred in less than 10 years at some sites (Allison et al., 1986) and is linked to regional shifts in water availability and temperature gradients (Booth et al., 2012; Foster et al., 2006; Haas and McAndrews, 1999; Shuman et al., 2023). Initial hypotheses that a pest or pathogen such as hemlock looper (Bhiry and Filion, 1996; Davis, 1981; Anderson et al., 1986) caused the hemlock decline have not been supported by recent investigations (Oswald et al., 2017), although insect remains are scarce in lacustrine archives. Understanding the causes of the hemlock collapse is outside the scope of this paper; however, this paper





shows its importance, in that a single-species collapse fundamentally altered the functional composition, ecosystem phenology, and land cover of the NEUS/SEC for thousands of years.

Among summergreen taxa, these REVEALS reconstructions indicate a strong growth in *Acer* (maple) cover in the NEUS/SEC until 4 ka and declines thereafter. *Acer saccharum* (sugar maple) is probably the dominant taxon driving this curve, with *A. rubrum* (red maple) increasing in the late Holocene (Finkelstein et al., 2006). *Quercus* (oak) abundances were high between 9 and 4.5 ka, then steadily declined, while *Betula* (birch) abundances remained relatively stable. *Fagus grandifolia* (American beech) abundances continued to steadily increase throughout this period until 3 ka, then began declining after 1.5 ka, along with *Tsuga canadensis*, while *Abies balsamea* abundances increased. Disturbance-related taxa and indicators of open vegetation such as *Ambrosia* (ragweed) and *Rumex* (sorrel, not shown) begin increasing at ca. 0.35 ka (1600 CE). These late-Holocene changes in forest composition can be plausibly attributed to regional cooling (explaining the increase in *Abies balsamea*) and perhaps also intensified human land use and disturbance, with the relative importance of these drivers varying at subregional scales and among taxa (Oswald et al., 2020; Mottl et al., 2021).

An intriguing feature of these REVEALS reconstructions is the inference of *Abies balsamea* and *Acer* spp. as the most common evergreen and summergreen tree taxa in the NEUS/SEC, given that *Picea*, *Pinus*, and *Quercus* are more abundant in pollen and macrofossil records and prior site-level and regional syntheses of Holocene pollen records have emphasized their dynamics (Jackson et al., 1997; Jackson and Whitehead, 1991; Payette et al., 2022; Spear et al., 1994). Witness-tree data in the NEUS also indicate that *Fagus* and *Quercus* were the most abundant broadleaved taxa at time of European settlement (Thompson et al., 2013). One possible reason for the higher levels of *Abies* and *Acer* reported here is that our NEUS/SEC domain extends a bit farther north than prior reconstructions that have focused more on central and southern New England. A second possibility is that the parameterizations for *Abies* and *Acer* are incorrect, causing the coverages of these taxa to be overestimated (see Discussion).



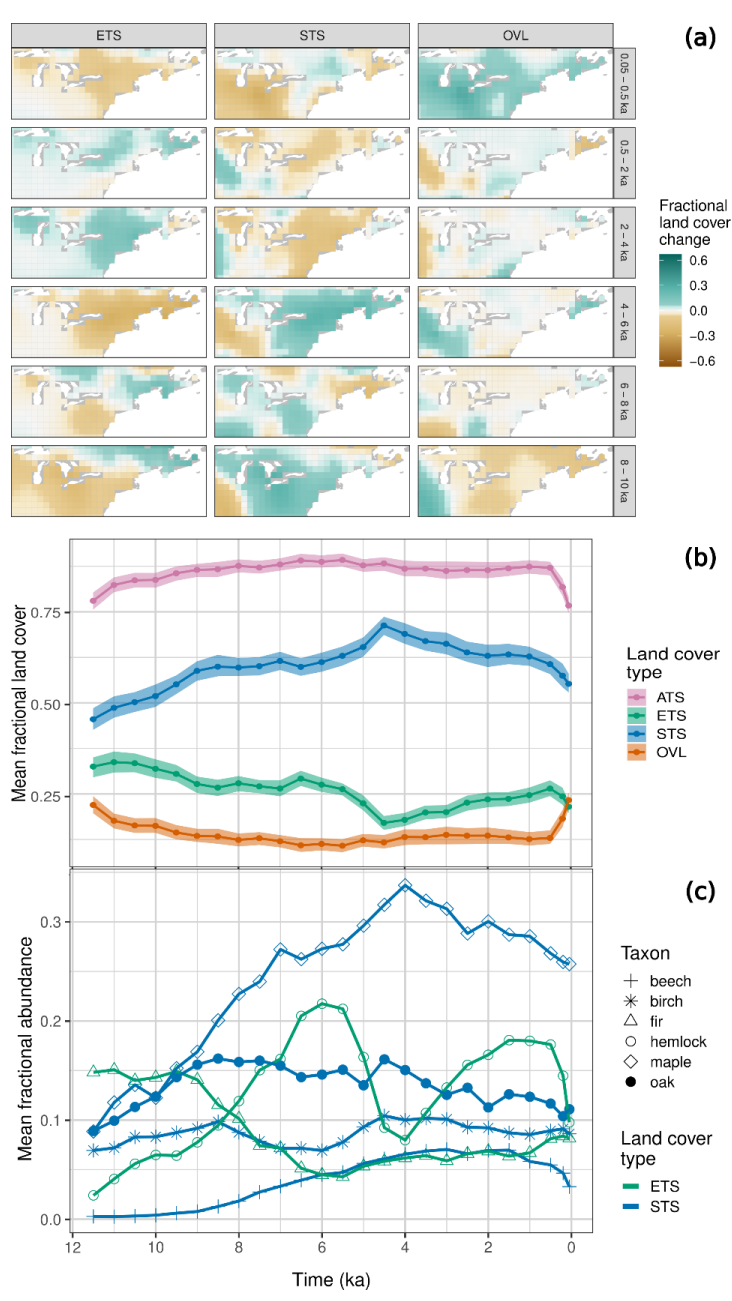


Figure 4: (a) Land cover anomaly maps for the northeastern US and southeastern Canada (NEUS/SEC) case-study region. Maps show the anomalies in fractional cover for each land cover class for pairs of indicated time intervals. Spatial resolution is 1°x1° and time units are ka.

(b) Holocene trends in the mean relative cover of the three land cover types (ETS, STS, OVL)





and the ATS sum for the uninterpolated REVEALS grid cell estimates across the NEUS/SEC region. (c) Holocene trends for the REVEALS abundance estimates for the six most commonly
 occurring taxa in the region. Line color indicates assignment of individual taxa to land cover types. For taxon-level maps, see Supp. Fig. 6.

3.3.2 Eastern Canada (ECAN)

428 In Eastern Canada (ECAN), immediately north of the NEUS/SEC, evergreen trees and shrubs expanded across the entire region until 4 ka, with slower and more spatially heterogeneous expansion of evergreen 430 cover between 4 and 2 ka (Fig. 5a, Supp. Fig. S7). After 4 ka, open vegetation expanded (Fig. 5a, 5b). This expansion of evergreen trees and shrubs can be traced to separate phases of expansion for Abies 432 balsamea and Picea, with A. balsamea expansion mostly between 11.5 and 7.5 ka (in the southern portion) and Picea expansion mostly between 7.5 and 3 ka, across the area and especially in the central 434 portion (Fig. 5c, Supp. Fig. S8). Increasing Cyperaceae abundance after 3.5 ka signal the expansion of forest-tundra. Major hardwood summergreen taxa include Betula and Alnus. Alnus abundances expanded 436 until 6 ka, then slowly declined, while birch abundances expanded between 8.5 and 6 ka, then also declined. These declines in Alnus and Betula after 6 ka co-occurred with expansions of Picea and 438 Cyperaceae, suggesting that the regional vegetation shifted from more of a mixed forest or woodland in the early Holocene, to evergreen coniferous forest, forest-tundra, or tundra in the middle to late 440 Holocene. Note that Populus is not included in these REVEALS reconstructions, but it is an important taxon in ECAN (Peros et al., 2008), and its omission may cause an underestimate of summergreen cover. 442 These vegetation changes in ECAN can be attributed to a combination of deglaciation, changing temperatures, and fire history. The Laurentide Ice Sheet collapsed at 8.4 ka and the last remnants of the 444 Labrador Dome disappeared from northern Quebec by 5.7 ka (Dalton et al., 2020). The replacement of open land by forest cover during the early Holocene was driven primarily by increases in evergreen trees 446

Labrador Dome disappeared from northern Quebec by 5.7 ka (Dalton et al., 2020). The replacement of open land by forest cover during the early Holocene was driven primarily by increases in evergreen trees and shrubs. The open forests at this time lack modern analogues and varied spatially in taxonomic composition, with more fir and birch to the east and spruce toward the west (Richard et al., 2020). By 7.5 ka, closed forests developed in response to warmer temperatures. This was followed by a decrease in summergreen taxa in the southern portion of the boreal forest as well as a decline in fir in the lichen woodland and feathermoss forest toward the west (Fréchette et al., 2021; Richard et al., 2020). In the lichen woodlands of the north, shrub birch and paper birch decreased after 6ka, although remaining high in the southwest (Fréchette et al., 2018). Near treeline, spruce forests were more open between 7 and 4 ka, with *Alnus* and shrub *Betula* more abundant (Fréchette et al., 2018; Gajewski, 2019). In ECAN, spruce abundances reached a maximum between 4 and 2 ka (Fréchette et al., 2018), with the southern portion of the forest tundra becoming lichen woodland at this time. After 2 ka, *Picea* abundances at northern sites

https://doi.org/10.5194/cp-2024-6 Preprint. Discussion started: 20 February 2024 © Author(s) 2024. CC BY 4.0 License.



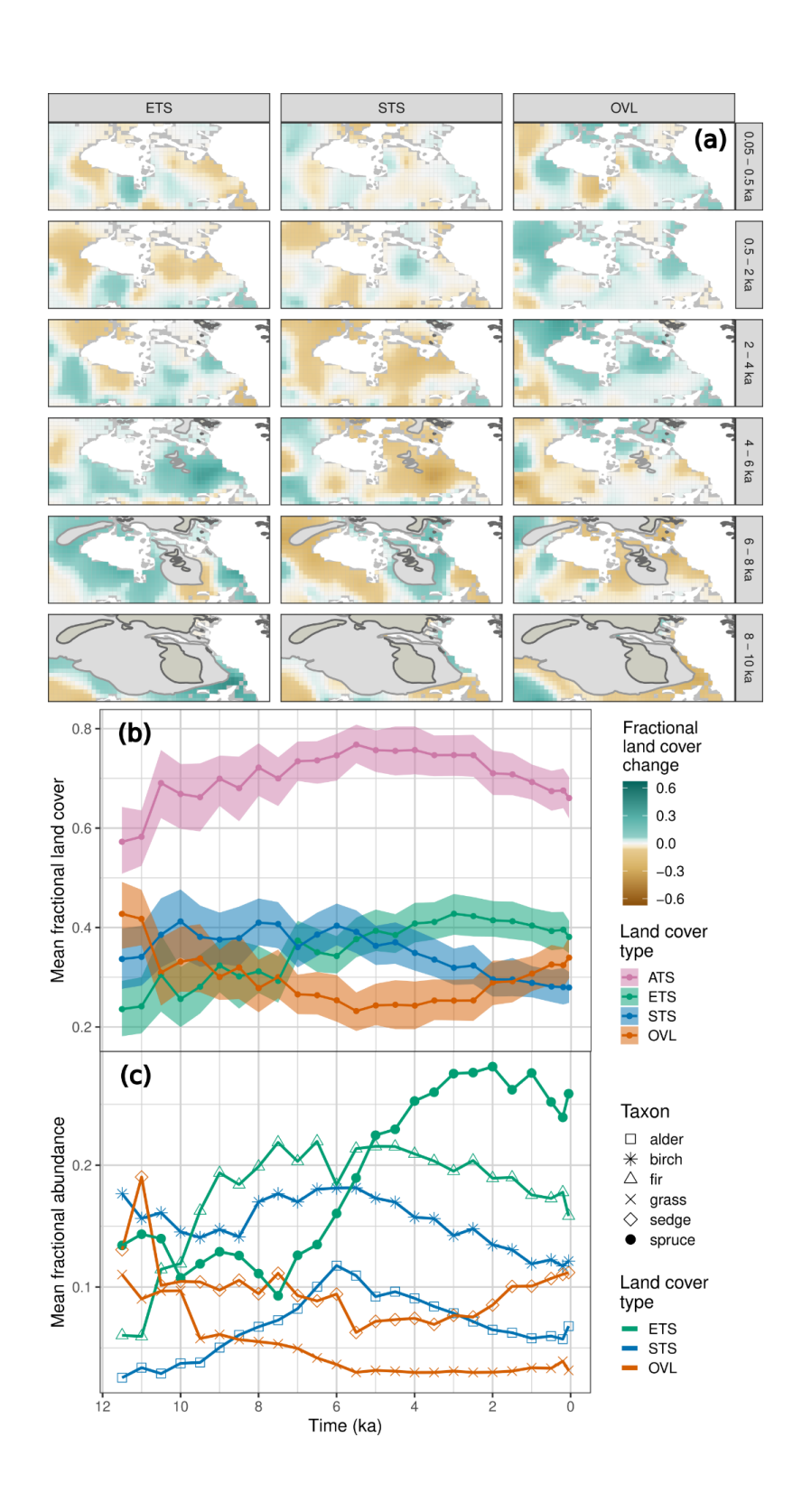


declined and open lands increased in response to cooling, but the timing and rate of *Picea* losses varied among sites and is governed in part by fire history (Gajewski et al., 2021; Gajewski, 2019).

458







(Anderson et al., 2019).

490





460 Figure 5: (a) Land cover difference maps for ETS, STS, and OVL for the eastern Canada (ECAN) case study. (b) Holocene trends in the mean relative cover of the three land cover types (ETS, STS, OVL) and 462 the ATS sum for the uninterpolated REVEALS grid cell estimates across the ECAN region. (c) Holocene trends for the REVEALS abundance estimates for the six most commonly occurring taxa in the region. 464 For both panels, figure conventions follow Figure 4. For taxon-level maps, see Supp. Fig. 8. 466 3.3.3 Western Canada and Alaska (WCAN/AK) In western Canada and Alaska (WCAN/AK), evergreen trees and shrubs rapidly expanded between 11 468 and 8 ka, while the coverage of summergreen trees and shrubs and open lands decreased (Fig. 6a, 6b, Supp. Fig. S9). Most of Alaska was not glaciated during the Last Glacial Maximum; however, much of 470 western Canada, the Brooks Range in Alaska, and south-coastal Alaska were covered by ice (Dalton et al., 2020). Evergreen tree species such as Picea glauca (white spruce) persisted in this region in local 472 microrefugia (Anderson et al., 2006), then expanded their ranges during end-Pleistocene warming and deglaciation. Other evergreen taxa such as Pinus contorta expanded northward with deglaciation 474 (MacDonald and Cwynar, 1991). Trends in taxon abundances differ substantially between the western and eastern subregions (Fig. 6c, Supp. Fig. S10). In the eastern subregion, changes in taxon abundances 476 were muted, with a modest expansion in Picea and Tsuga between 11.5 and 7.5 ka, and a slow decline in Betula between 10 and 6 ka. Tsuga (mostly Tsuga heterophylla; western hemlock) occurs primarily along the coast, was abundant along the south coastal areas by 11 ka (Lacourse et al., 2012; Lacourse and 478 Adeleye, 2022), arrived by 9.5 ka into southeast Alaska (Hansen and Engstrom, 1996; George et al., 480 2023), increased in abundance along the south-coastal areas by 8 ka, and then expanded during the midto late Holocene into south-central Alaska (Anderson et al., 2017) and the inland mesic forests of British 482 Columbia (Rosenberg et al., 2003; Gavin et al., 2021). In the western part of this domain (mainly Alaska), changes in summergreen hardwood (mostly shrub) taxa predominate, with a major expansion of 484 Alnus between 11.5 and 6.5 ka (Anderson and Brubaker, 1994; Cwynar and Spear, 1995), and a modest expansion of Betula between 11.5 and 9 ka. These expansions were accompanied by declines in Poaceae 486 and Cyperaceae, with continued decline in Cyperaceae until 6 ka. Picea abundances steadily increased until 4 ka. The net effect was a decline in open vegetation and expansion of evergreen and summergreen 488 trees and shrubs during the early to middle Holocene, with apparent region-wide stability after 4 ka

21





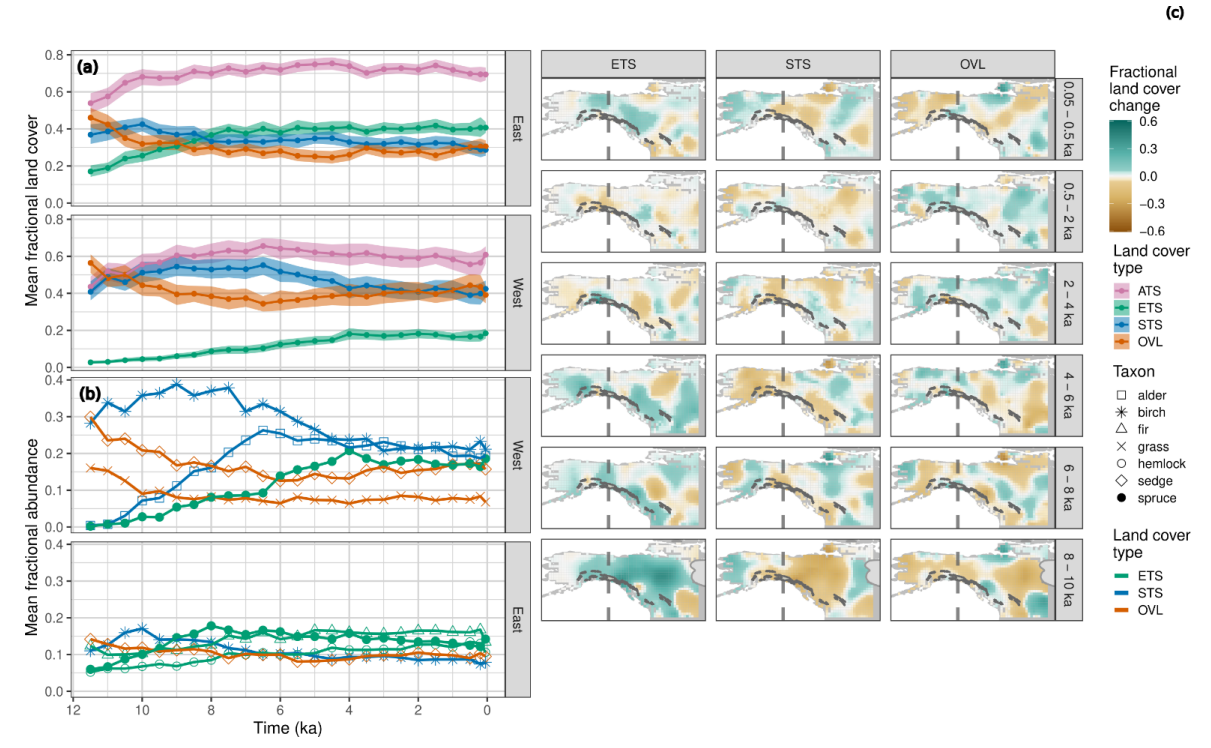


Figure 6: (a) Land cover difference maps for the western Canada / Alaska (WCAN/AK) case study region. (b) Holocene trends in the mean relative cover of the three land cover types (ETS, STS, OVL) and the ATS sum for the uninterpolated REVEALS grid cell estimates across the WCAN/AK region, with grid cells averaged separately for eastern and western subregions (dividing line shown in (a) as vertical dashed line). (c) Holocene trends for the REVEALS abundance estimates for the six most commonly occurring taxa in the region, with grid cells averaged separately for eastern and western subregions. For both panels, figure conventions follow Figure 4. For taxon-level maps, see Supp. Fig. 10.

3.3.4 Pacific Coast, Cascade, and Sierra Nevada Ranges (PCCS)

In contrast to the other regions, evergreen trees have dominated much of the land cover in the PCCS region since 12 ka (Fig. 7a, 7b, Supp. Fig. S11). In the northern subregion (often referred to as the Pacific Northwest), the proportions of cover types were fairly constant until 9 ka, after which summergreen and open land declined until 6 ka (Fig 7a, 7b). However, taxon-level changes were very dynamic. From 11.7 to 10.5 ka, the REVEALS-estimated abundance of *Pseudotsuga menziesii* (Douglas-fir) more than doubled, reflecting its arrival, expansion, and northward migration (Gugger and Sugita, 2010), and replacing true firs (*Abies*) and *Picea* (Fig 7c, Supp. Fig. S12). In the coastal ranges, frequent forest fires in the early Holocene contributed to a *Pseudotsuga-Alnus rubra* association in the mountains (Gavin et



534

536

538

540

542



512 open-land pollen indicators declined from 8 to 6 ka (Fig 7b), replaced by shade-tolerant Abies, Tsuga, and Cupressaceae, which is mostly western redcedar in this region (Fig. 7b) (Lacourse, 2009; Gavin et al., 514 2013; Worona and Whitlock, 1995). After 6 ka, the overall abundance of conifer taxa remained constant (Fig 7a, 7b), although the proportion of hemlock and cedar increased steadily through the late Holocene 516 while Pseudotsuga declined, consistent with less fire and the persistence of old-growth forest (Whitlock, 1992; Lacourse and Adeleye, 2022), until the logging of the last century, which manifested as a decline in 518 conifer and increase in summergreen and open land in the coastal forests (Fig. 7a) (Davis, 1973; Whitlock et al., 2018). 520 The most common taxon in these REVEALS reconstructions, Abies, varied little over the last 9 ka, but this genus represents several shade-tolerant species (A. lasiocarpa [subalpine fir], A. grandis 522 [grand fir], A. amabilis [Pacific silver fir], A. procera [noble fir]) that collectively are common throughout the region. As noted for the NEUS/SEC, the reconstructed values of Abies are likely too high, because 524 REVEALS estimate of fall speed is overestimated. Pinus also represents several species and was most abundant in the dry eastern areas where it was consistently abundant during the Holocene (Minckley et 526 al., 2007). Pseudotsuga and Larix have indistinguishable pollen morphologies and are therefore grouped in the reconstructions; however, *Larix* is limited to the eastern edge of this region. 528 The southern subregion (the Sierra Nevada, Klamath Mountains and California Coast ranges and interior Great Basin) supported roughly equal amounts of conifer forest and open land that overall had 530 minor relative changes over the Holocene (Fig. 7a). Summergreen trees and shrubs have been infrequent contributors to land cover in this subregion. At the taxon-level, Abies is again the most common 532 component of reconstructed evergreen land cover across the region, although its abundance may be overrepresented in this parameterization of REVEALS (Fig. 7b). Pinus and Quercus were most abundant

al., 2013; Long et al., 1998, 2007) and an oak savanna (not shown) that was common in the lowlands (Walsh et al., 2008, 2010; Giuliano and Lacourse, 2023). Summergreen taxa (mostly *Alnus rubra*) and

2008; Brugger and Rhode, 2020; Minckley et al., 2007; Thompson, 1992). Note, however, that desert, steppe, and other open-land arid ecosystems are likely to be underrepresented in these reconstructions, due to a scarcity of dryland sites.

local expansion of alpine meadows and wetlands or expansion of steppe more broadly (Mensing et al.,

in the early Holocene, forming open forests and woodlands, especially in the Klamath Mountains and Sierra Nevada (Anderson, 1996; Briles et al., 2008) fire-prone forests east of the Cascade Range (Walsh

et al. 2015);. Most of the eastern portion of this subregion is the Great Basin shrub steppe, where the few pollen records that exist are from high-elevation sites and low-elevation wetlands that are sensitive to

fluctuating water tables, recorded as large fluctuations in Cyperaceae pollen. Increases in open-land cover taxa (Cyperaceae, Poaceae, Asteraceae) between 10-7.5 ka and after 3 ka in this region may reflect either





546

548

550

552

554

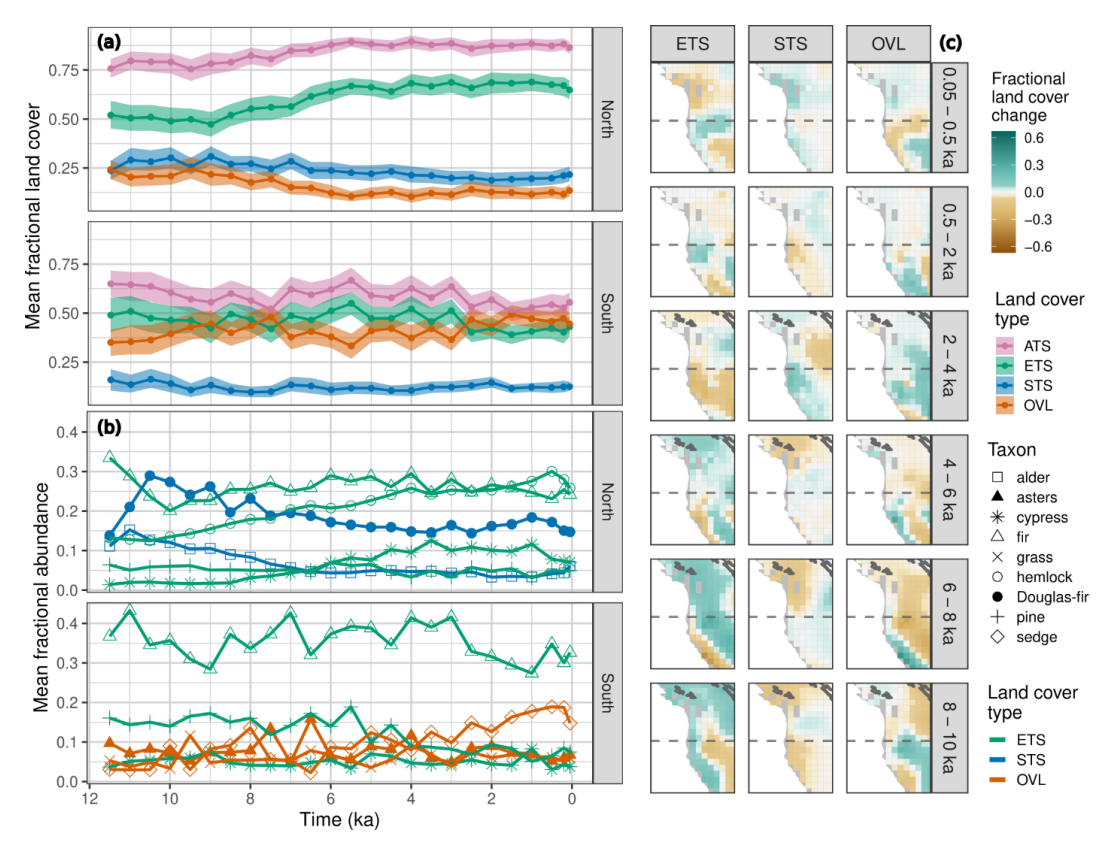


Figure 7: (a) Land cover difference maps for the Pacific Coast, Cascade and Sierra Nevada (PCCS) case study region. (b) Holocene trends in the mean relative cover of the three land cover types (ETS, STS, OVL) and the ATS sum for the uninterpolated REVEALS grid cell estimates across the PCCS region, with grid cells averaged separately for northern and southern subregions (dividing line shown in (a) as vertical dashed line). (c) Holocene trends for the REVEALS abundance estimates for the six most commonly occurring taxa in the region, with grid cells averaged separately for northern and southern subregions. For both panels, figure conventions follow Figure 4. For taxon-level maps, see Supp. Fig. 12.

4. Discussion

4.1 Drivers of Holocene land cover change in North America: scaling from taxon-level regional dynamics to continental-scale trends





These continental-scale Holocene changes in land cover (Figs. 2-3) are an emergent outcome of the individualistic plant responses to deglaciation and multiple environmental changes, including seasonal
temperatures, effective moisture, atmospheric carbon dioxide, soil development, fire and other disturbance regimes, and, at some locations during the late Holocene, human land use. As shown here
(Figs. 4-7), this interplay differed spatially across North America, often with opposing trends (e.g. simultaneous increases in evergreen cover in some regions and decreases elsewhere) that partially offset
at the continental scale.

The first-order continental-scale drivers of Holocene land cover change in North America were changing climates and the retreat and disappearance of the Laurentide Ice Sheet, particularly during the early Holocene (11.7 to 7.5 ka) and lasting until 5.7 ka, with the disappearance of remnant ice in the Labrador Dome in northern Quebec (Dalton et al., 2020). Deglaciation and an overall increase in land availability explains why all land cover types show an increase in area-weighted cover during the early Holocene, with evergreen taxa showing the greatest gain (Fig. 3). Continental temperatures also closely tracked the decline in ice area (Marsicek et al., 2018), and vegetation responded to both factors.

Superimposed upon the early-Holocene increase in area-weighted cover for all PFTs are gains and losses for each PFT at subregional scales (Figs. 4-7), which can be linked to climate-driven changes in plant abundances at local to landscape scales that scaled upwards to continental-scale shifts in plant

abundances at local to landscape scales that scaled upwards to continental-scale shifts in plant distributions, with both within-range shifts in dominance and leading-edge and trailing-edge range dynamics for individual plant taxa (Payette et al., 2022; Williams et al., 2004; George et al., 2023; Dallmeyer et al., 2022; Anderson et al., 2017).

Leading-edge dynamics and range expansion of tree taxa appear to have been primarily controlled by the increasing availability of deglaciated land area, end-Pleistocene warming, the declining influence of ice sheet on regional climates and moisture availability (Alder and Hostetler, 2015; Bartlein et al., 2014), and on-going expansion of plant taxa into areas of increased climate suitability (Payette et al., 2022; Williams et al., 2004; George et al., 2023; Dallmeyer et al., 2022). Declining ice extent favored moisture advection into eastern areas where most of the increase in summergreen tree taxa took place and reduced it in midcontinental North America, where most of the open vegetation increase developed (Shuman and Marsicek, 2016; Shuman et al., 2002; Liefert and Shuman, 2020). These changes in the patterns of moisture availability simultaneously favored the large increase from 10 to 6 ka in summergreen trees and shrubs in eastern North America south of the former Laurentide Ice Sheet and the increase in open land in the mid-continent (Supplementary Fig. 2-3).

Declines in abundance and trailing-edge dynamics of tree taxa were likely governed by a combination of declining climate suitability and, in some places, fire regimes, in which many local populations failed to re-establish after one or more fire events. For example, in the high northern latitudes



624

and total summer warmth (see Section 4.2).



first to declining summer insolation and temperatures, caused by precessional changes in the Earth's orbit 594 (Payette, 2021), but at local to landscape and centennial scales, loss of forest cover was asynchronous and caused by individual fire events (Payette et al., 2008; Gajewski et al., 2021). Similarly, in the southern 596 Great Lakes region and NEUS, the late-Pleistocene to early Holocene transition from conifer-dominated forests and parklands to summergreen forests was driven by rising temperatures and changes in effective 598 moisture (Shuman et al., 2002; 2019), but accelerated locally by intensified fire regimes, with the timing and rate of conversion varying among sites (Jensen et al., 2021; Clark et al., 1996). The expansion and 600 then retreat of the Great Plains prairies (Fig. 4) was driven by early Holocene aridification and middle- to late-Holocene increases in moisture availability, while fire may have facilitated prairie expansion, but 602 delayed its retreat (Williams et al., 2009; Nelson et al., 2006; Umbanhower et al., 2006). Of course, throughout North America, forests and fire dynamically co-existed and interacted during the Holocene 604 (Iglesias and Whitlock, 2020; Kelly et al., 2013), so whether fire causes transformative shifts in ecosystem type depends on its synergistic interactions with directional changes in climate and other 606 factors (Napier and Chipman, 2021). Regardless of the role of fire or other disturbances, regional shifts in temperature and moisture availability are usually the first-order predictors of Holocene changes in 608 vegetation composition (Dean et al., 1984; MacDonald, 1989; Calder and Shuman, 2017; Shuman et al., 2004; Nelson et al., 2006). 610 The relative proportion of evergreen and summergreen cover types may have been affected by changes in the length and intensity of the growing season during the Holocene, which is regulated by 612 precessional variations in insolation. In particular, the broad peak in summergreen tree cover between 8.5 and 3.5 ka (Fig. 3) is consistent with the hypothesis that summergreen tree and shrub abundances in North 614 America are partially regulated by summer insolation and temperatures (Delcourt and Delcourt, 1994; Williams et al., 2001). Summer insolation reached higher peak intensity but has a shorter seasonal 616 duration in the early Holocene than during the late Holocene (Huybers, 2006; Jackson et al., 2009), which may have favored plants with summer deciduous phenology that could more effectively exploit available 618 energy during a briefer but more intense growing season (Delcourt and Delcourt, 1994; Williams and Jackson, 2007; Edwards et al., 2005). Indeed, pollen-reconstructed and CCSM3-simulated changes in 620 growing-degree days also peaked during the mid-Holocene when forest cover was greatest, and several millennia after peak summer temperatures, likely because of differential responses of maximum summer 622 temperatures and total growing season warmth to orbital and other forcings (Marsicek et al., 2018). This may in turn suggest a seasonal-scale feedback loop between summer insolation, deciduous phenology,

of Quebec and Labrador, the expansion of open lands over the last three thousand years can be attributed





626 upon land cover and understanding the interactions among past climate change, fire regime, and human land use is a highly active area of research. Rates of vegetation change worldwide began to increase 628 between 4.6 and 2.9 ka (Mottl et al., 2021), consistent with growing intensification and extent of land use (Stephens et al., 2019). The 7 to 10 ppm decrease in global CO₂ between 1570 and 1620 CE has been 630 attributed to the land abandonment and reforestation due to mass mortality of Indigenous populations in the Americas, caused by the spread of multiple pathogens (Lewis and Maslin, 2015). The best evidence 632 for dense human populations and extensive land clearance in the Americas comes from Central and tropical South America (Islebe et al., 1996; McMichael, 2020). 634 In North America, the effects of human land use prior to EuroAmerican settlement are detectable at some sites, but are not easily detected at the regional to continental scales addressed here. In North 636 America, the distribution of radiocarbon dates from archaeological contexts suggest that population levels remained relatively low and increasing slowly until ~7 ka, with further increases between 7 and 2 ka, and 638 then rapidly increased after 2 ka (Peros et al., 2010). Indigenous cultures in North America clearly engaged in activities that, in some areas, modified the composition and structures of forested and 640 unforested landscapes for millennia (Ellis, 2021; Delcourt et al., 1986; Leopold and Boyd, 1999; Munoz et al., 2014). In densely populated regions, such as lands of the Iroquois Confederacy, southern Ontario, or the Cherokee Nation, Cahokia and the American Riverbottom, land use altered vegetation structure and 642 composition at local to landscape scales, through management of fire regimes (Roos et al., 2018; 644 Anderson and Carpenter, 1991), land clearance for agricultural crops (McAndrews and Turton, 2007), and silviculture, e.g. favoring the spread of nut-bearing trees (Munoz et al., 2014; Black et al., 2006). In 646 western North America, the effects of anthropogenic activity on vegetation and fire is an active area of research, with several paleoecological studies indicating changes consistent with human influences on 648 forest composition (Walsh et al., 2015; Knight et al., 2022; Lacourse et al., 2007). Because the scale of human action was strongest at local to landscape scales and varied in intensity within and among regions, 650 its detection often requires highly-focused, local- to regional-scale studies (Oswald et al., 2020; Roos, 2020; Lacourse et al., 2007; Knight et al., 2022; Munoz and Gajewski, 2010). These studies clearly 652 indicate a high intersite variance in the level and detectability of human impact. At the continental scale, Gajewski et al. (2019) did not find clear correlations between human population abundance and pollen 654 abundance, including taxa of economic use or disturbance taxa, and concluded impacts were at local to regional scales. Thus, at the regional to continental scales considered here, it is an open question whether 656 the rich relationships and diverse activities engaged by communities within their homelands led to

detectable changes in land cover types. We expect that pollen-based land cover reconstructions will

During the late Holocene, human land use in the Americas intensified, with increasing effects



660

662

664



continue to contribute to interdisciplinary approaches to address anthropogenic fire and land cover change during the Holocene (Snitker et al., 2022).

In contrast, after EuroAmerican arrival and expansion from 1492 onwards, North American ecosystems were massively transformed (Stegner and Spanbauer, 2023) by multiple anthropogenic processes. These include widespread forest conversion to agricultural and pastoral lands, intensive forest harvesting, massive hydrological change through dam construction and wetland drainage, introduction of exotic species and pests, and both greatly increased fire activity and fire suppression (Klein Goldewijk et al., 2011; Foster and Aber, 2004).

666

4.2 Biophysical vegetation-atmosphere feedbacks to Holocene climates

668 4.1.1 Holocene vegetation-atmosphere feedbacks: prior work and need for data constraints This paper and the other REVEALS-based reconstructions for the Northern Hemisphere (Githumbi et al., 670 2022c; Li et al., 2020) are now laying the foundation for a next generation of Holocene vegetationatmosphere research with well-constrained land surface data. Many studies have explored the potential 672 impacts of vegetation-atmosphere feedbacks on Holocene climate dynamics at hemispheric to global scales, but these studies have generally not employed well-constrained land cover reconstructions. 674 Treeline shifts have been recognized as an important regulator of Holocene vegetation-atmosphere feedbacks in the high northern latitudes (TEMPO (Testing Earth System Models with Paleo-676 Observations), 1996). Earth system model experiments with prescribed vegetation scenarios have shown that, in the northern latitudes (45-90N), changes in forest cover are the largest contributor to changes in 678 net land surface radiation through snow masking and effects on surface albedo (Bathiany et al., 2010). In mid-Holocene atmosphere-vegetation model simulations, strong snow masking resulted in warming three 680 times higher than those with weak snow masking (Otto et al., 2011). Additionally, empirical estimates of surface-albedo feedbacks in high latitudes are stronger than predicted by climate models (Hogg, 2022). 682 More recent work has highlighted the importance of the type and density of forest cover in determining the albedo feedback and magnitude of snow masking (Loranty et al., 2014; Alessandri et al., 2021). 684 Hence, because snow masking and surface albedo is an important regulator of surface-atmosphere feedbacks in climate models, it is also an important source of uncertainty in Holocene climate 686 simulations, because of the limited availability of well-constrained reconstructions of past changes in vegetation type, structure, and density. Vegetation structure and topographic complexity also jointly 688 govern surface roughness, which affects lower atmosphere temperature, humidity, wind speed, and soil moisture (Bonan, 2015) and is the dominant land-cover influence on micrometeorological processes 690 (Chen and Dirmeyer, 2016). This new generation of LandCover6k vegetation reconstructions thus





promise to sharpen our understanding of the role played by surface-atmosphere feedbacks in Holocene climate dynamics, with first results from Europe already underway (Strandberg et al., 2022b).

The Holocene Conundrum has been a major focus of paleoclimatic research over the last decade

4.1.2 Assessing recent modeling studies of the Holocene conundrum

(Kaufman and Broadman, 2023; Liu et al., 2014), and recent research has invoked vegetation-atmosphere feedbacks to resolve this conundrum (Thompson et al., 2022). The Holocene Conundrum involves a discrepancy between proxy-based reconstructions of global temperature changes, mostly based on marine records, which indicate a mid-Holocene maximum and mid- to late-Holocene cooling (Marcott et al., 2013), while transient model simulations show small but steady warming throughout the Holocene (Liu et al., 2014). Many explanations for this discrepancy have since been proposed (Kaufman and Broadman, 2023). Recent prescribed-vegetation experiments in climate models produce an early Holocene warming to a Holocene Thermal Maximum, followed by cooling towards the pre-industrial Holocene (Thompson et al., 2022), consistent with paleoclimatic proxies. Conversely, experiments that include drivers such as dust, ice cover, orbital forcing, and greenhouse gasses without accounting for Northern Hemisphere vegetation changes do not result in a mid-Holocene thermal maximum (Thompson et al., 2022).

Our reconstructions suggest, however, that for North America, the prescribed vegetation maps used by Thompson et al (2022) overstate the magnitude of Holocene vegetation change. These prescribed-vegetation experiments for 9 and 6 ka fully replace all C₃ grasses with boreal forest for all locations north of 50N (Thompson et al., 2022, Supp. Fig. 7B). This pattern is qualitatively consistent with the early Holocene afforestation reported here (Fig. 2) but is inconsistent with the demonstrated persistence of tundra throughout the early and middle Holocene, particularly in WCAN/AK (Figs. 2, 6) and Canadian High Arctic (Fig. 2). Similarly, the prescribed full replacement of C3 grasslands with temperate deciduous forest for the 9 and 6 ka experiments (Thompson et al., 2022, Supp. Fig. 7B) is inconsistent with clear palynological evidence of the establishment of the Great Plain grassland by the early Holocene and prairie expansion during the early to middle Holocene (Fig. 2, Supp. Fig. 1) (Williams et al., 2009a). Hence, the Thompson et al (2022) simulations should be viewed as useful experiments that show the potential sensitivity of Holocene climates to large vegetation changes, but these experiments likely overestimate the contribution of vegetation feedbacks to resolving the Holocene Conundrum.

4.1.3 Understudied Holocene vegetation-atmosphere feedbacks in North America

Our reconstructions also highlight several major features of North American vegetation dynamics that may have underappreciated effects on Holocene vegetation-atmosphere feedbacks and climate dynamics at regional to continental scales. First, the mid-Holocene decline and recovery of *Tsuga*





756

758

726 dynamics can drive fundamental changes in vegetational structure. Although the patterns and drivers of the T. canadensis decline have been extensively studied (Oswald and Foster, 2012; Oswald et al., 2017; 728 Booth et al., 2012; Foster et al., 2006), the effects of the T. canadensis decline on Holocene climates are unknown. As the dominant evergreen conifer of cool-temperate eastern North America, the decline of T. 730 canadensis at ca. 5 ka is the primary driver of the loss of ETS between 6 and 4 ka, while the gradual recovery of T. canadensis after 5 ka drives the corresponding increase of ETS (Fig. 4). This shift in 732 dominance between summergreen and evergreen trees and shrubs, in turn, regulates the overall albedo of the land surface and particularly its seasonal range. During times of foliage, summergreen forests can 734 have more than twice the albedo of evergreen forests (Hollinger et al., 2010). Summergreen forests also exhibit much greater seasonal variability in albedo, with maximum values in full foliage being 20-50% 736 larger than annual lows. Second, the peak in summergreen tree cover between ca. 8.5 and 4.5 ka (Fig. 2) may indicate a 738 seasonal-scale positive feedback loop between summer insolation, summergreen phenology, and summer temperatures. Studies have suggested that the late-Pleistocene to early-Holocene peak in summer 740 insolation favored summergreen phenology and carbon acquisition strategies over evergreen strategies (Delcourt and Delcourt, 1994; Williams and Jackson, 2007). Studies from the Pacific Northwest and 742 Alaska also show a peak in Alnus and other summergreen tree and shrub taxa during the early Holocene (Fig. 7c), coincident with the summer insolation maximum and local maxima in temperature (Gavin et al., 744 2013; Edwards et al., 2005; Whitlock, 1992). This climate-driven response, in turn, may have increased the seasonal range of albedo and surface temperatures, thereby further favoring summergreen strategies. 746 This summergreen feedback might have also contributed to some summer cooling, due to the higher summer albedo of summergreen trees (Hollinger et al., 2010). As an alternative hypothesis, Herzschuh, 748 (2020) suggested that the Eurasian distribution of evergreen spruce-dominated and deciduous larchdominated evergreen forests was due to historical contingencies and alternate stable states. Although 750 many studies have explored the effect of early to middle Holocene afforestation on vegetation feedbacks in the northern latitudes (Brovkin et al., 2009; TEMPO (Testing Earth System Models with Paleo-752 Observations), 1996), to our knowledge no paper has yet focused specifically on the seasonal feedback effects associated with shifting proportions of summergreen and evergreen trees and shrubs.

canadensis (eastern hemlock) in the northeastern United States is an example of how single-species

4.3 Uncertainties and limitations in pollen-vegetation model reconstructions

Land cover reconstructions from pollen rely upon a variety of pollen-vegetation models (PVMs), some of which have well-understood limitations and uncertainties, and some of which are newer and are still being studied. The REVEALS PVM used here is has been widely adopted (e.g. Li et al., 2020; Githumbi et al.,





2022c; Serge et al., 2023; Azuara et al., 2019; Hoevers et al., 2022) because it represents some of the 760 taxon-level processes governing pollen production, transport, and representation (Sugita, 2007a; Prentice, 1985). However, processes such as atmospheric transport are simplified (Jackson and Lyford, 1999a) and 762 key parameters such as pollen productivity estimates (PPEs) carry uncertainties (Wieczorek and Herzschuh, 2020; Broström et al., 2008; Hayashi et al., 2022) that translate to uncertainties in fractional-764 weighted land cover area. Most PPE estimates are generated from models fitted to spatial networks of vegetation surveys and surface pollen samples, and these PPE estimates depend strongly on models of 766 pollen dispersal (Theuerkauf et al., 2012). Such issues may explain some of the surprising aspects of the reconstructions presented here. For 768 example, reconstructed Acer cover in the NEUS/SEC (Fig. 4c) is high compared to settlement-era estimates from witness trees and land surveys (Thompson et al., 2013; Paciorek et al., 2016). Similarly, 770 reconstructed cover of Abies in both the NEUS/SEC and PCCS is higher than expected (Figs. 4c, 7c). Abies and Acer are notoriously underrepresented in fossil pollen assemblages (Bradshaw and Webb, 772 1985), relative to independent surveys of tree abundance in the surrounding ecosystems, due to the low pollen productivity of maple trees relative to other taxa (Finkelstein et al., 2006; Liu et al., 2022) and high 774 fall speeds of Abies (Jackson and Lyford, 1999b). Hence, a key value of process-based PVMs, such as REVEALS, is the ability to correct for these known biases. However, REVEALS estimates are sensitive 776 to parameter choices and it is possible that the estimates of Abies and Acer are too high. There are few estimates of Abies fall speeds compared to other taxa, and the fall speeds used here from Wieczorek and 778 Herzschuh (2020) are similar to the values for Larix that initial testing indicated led to Larix overrepresentation. 780 REVEALS is not spatial or temporal in nature, so there is no representation of spatiotemporal dependencies among site-level reconstructions. REVEALS estimates of uncertainty are based on the total 782 number of pollen grains counted in a sample and the error associated with the PPEs, but do not include process uncertainty or uncertainty in other model inputs. The GMRF serves as a post-hoc interpolator to 784 generate spatio-temporally complete vegetation reconstructions, but this approach does not mechanistically represent the underlying processes that link pollen to vegetation. 786 To address these limitations with the REVEALS workflow (spatio-temporal incompleteness, input parameter uncertainty, and uncertainty quantification), other forms of PVMs have been developed. 788 ROPES uses pollen accumulation rates and REVEALS to estimate pollen productivity (Theuerkauf and Couwenberg, 2018). However, the dependence of ROPES on pollen accumulation rates may limit its 790 widespread utility. At many sites, pollen accumulation rates have high uncertainties due to variations in sedimentation rate, few radiometric dates and poor chronological controls, and spike counting 792 uncertainties (Perrotti et al., 2022). STEPPS is a Bayesian spatio-temporal PVM (Dawson et al., 2016,





2019b). While theoretically sound, STEPPS is computationally intensive and its estimates are dependent upon the density and quality of spatial forest compositional calibration datasets, limiting its applicability to regional-scale domains. Other spatial Bayesian models developed for high-resolution networks of pollen and vegetation data suggest that if the spatial site density is too low, STEPPS and similarly structured PVMs can over-estimate pollen dispersal distance (Liu et al., 2022).

4.4 Future work

With North American REVEALS-based reconstructions now in place, all middle- and high-latitudes in the Northern Hemisphere have quantitative reconstructions of Holocene land cover that are well constrained by dense networks of fossil pollen records (Githumbi et al., 2022a; Li et al., 2020). The reconstructions for North America and Europe also have estimates of uncertainty from the spatiotemporal GMRF model (Pirzamanbein et al., 2018a). This hemispheric coverage now enables the creation of a next generation of modeling scenarios, well-constrained by data, to explore land cover feedbacks in the Holocene climate system (Harrison et al., 2020). These land cover reconstructions also help identify places where new local-scale, site-based research are needed to better understand human impacts, better constrain land cover changes in areas of sparse data and high uncertainty, and better understand how local and taxon-level dynamics scale up to affect regional- to continental-scale vegetation and climate dynamics.

This work also underscores the critical need for more work to better constrain PPEs and fall speeds, particularly for North American plant taxa. The REVEALS estimates in this analysis appear to be particularly sensitive to the parameterizations for underrepresented taxa such as *Abies* and *Acer*.

Lastly, given the maturation of pollen-vegetation modeling as a field of study and the emergence of multiple PVMs, there is now the opportunity for intercomparison studies among PVMs and, perhaps, the development of ensemble-based inferences of past vegetation cover. There is a long history of methodological comparisons in pollen-based paleoclimatic inferences and paleoclimatology more broadly (Chevalier et al., 2020). Few systematic intercomparisons of PVMs yet exist (Roberts et al., 2018), although individual papers have discussed strengths and weaknesses of different modeling approaches (Liu et al., 2022; Theuerkauf et al., 2012). Initial efforts are underway to compare land cover reconstructions from REVEALS-GMRF to those from the Bayesian spatio-temporal model STEPPS. Moreover, given that ensemble-based approaches have been shown to have higher predictive ability in fields such as climate modeling and species distribution modeling (Deser et al., 2020; Bothe et al., 2013; Rangel et al., 2009; Thuiller et al., 2009), there is value in developing approaches for ensemble-based PVMs for past land cover inference.





5. Conclusions

Continental-scale changes in land cover in North America during the Holocene are the outcome of multiple interacting drivers operating over a range of temporal and spatial scales. For much of the Holocene (ca. 8 to 1.5 ka), the spatial configurations of continental-scale fractional forest cover were broadly stable. Major continental-scale trends included early Holocene afforestation, a middle-Holocene peak in the areal proportion of summergreen trees and shrubs, and a last-millennium increase in open land. These trends were powered by taxon-level dynamics that varied within and among regions. The regional dynamics can be attributed to individualistic postglacial shifts in the range and abundance of plant taxa driven by changing climates and increased land area after deglaciation; abrupt and large species-level events, such as the mid-Holocene collapse of eastern hemlock; and a shift from localized land use during the late Holocene to massive ecosystem transformation following EuroAmerican settlement. This work rejects the ideas of both pre-industrial forest stability and widespread major conversions in land cover type.

This work contributes to the LandCover6k initiative to produce continental- to global-scale reconstructions of Holocene land cover dynamics that are well-constrained by proxy data and are quantified using consistent methods. These REVEALS-GMRF reconstructions can help refine Holocene models of land use and land cover change, provide a foundation for comparisons among PVMs, indicate priority areas for future new site-level research, and establish realistic benchmark scenarios constraining and assimilating with Earth system model simulations of the interactions among Holocene climate, land cover, and anthropogenic change. Scaling up from these continental to hemispheric and global products will enable further testing of hypotheses about the drivers and feedbacks of Holocene land cover change. These reconstructions also highlight several potentially important but unstudied vegetation-atmosphere feedbacks, including the collapse of eastern hemlock at ca. 5 ka and a positive feedback loop between mid-Holocene peaks in seasonality of insolation, temperature, and vegetation phenology.

Comparison of the REVEALS-GMRF land cover reconstructions with those inferred from alternate PVMs is a research priority. REVEALS-GMRF depends on a suite of input variables that are both uncertain and exhibit spatial and temporal variation not accounted for in the model. Also, the use of a post-hoc Bayesian GMRF interpolation step means that uncertainty of reconstructions associated with these assumptions is not fully characterized.

Finally, this work emphasizes the importance of quantifying ecosystem processes and feedbacks between the land surface and climate system. Holocene land cover changes in North America are non-negligible and there is a pressing need to refine ecosystem models, in particular when those models are coupled within an Earth System model. The availability of well-constrained data products has been a





major barrier to this effort. Paleoecology and palynology are reaching a new level of maturity with

respect to advances in data discovery and accessibility, as well as development of consistent analytical
methods that permit interpretability of large-scale spatio-temporal change. Data assimilation experiments
that integrate these reconstructions into Earth System models have the potential to resolve major
questions in the field, such as the Holocene Conundrum and disentangling the effects of climatevegetation-human interactions upon Holocene vegetation and climate dynamics.

6. Code and data availability

- Code and data used in this workflow are publicly available at https://github.com/andydawson/reveals-na.

 The REVEALS-GMRF reconstructions are available at
- https://github.com/BehnazP/SpatioCompo_entireHolocene_NA. The description and implementation of the digitization of lake area is available at https://github.com/NeotomaDB/neotoma_lakes.

7. Author contributions

AD and JWW co-designed and co-wrote the paper, with AD leading on REVEALS analyses and figure
generation. MJG helped initiate this effort, led PAGES LandCover6k, and coordinated activities with
other continental-scale mapping groups. BP and JL assisted with the GMRF modeling and analyses,
while SG assisted with Neotoma data provision and digitization of lake size. RSA, AB, DF, KG, DG, TL,
TM, WO, BS, and CW all contributed new records to the North American Pollen Database in Neotoma
and assisted in data interpretation. All authors contributed to manuscript development and revision.

8. Competing interests

The authors declare that they have no conflict of interest.

9. Acknowledgments

This work is a contribution to the Past Global Change (PAGES) project and its working group
LandCover6k (https://pastglobalchanges.org/science/wg/former/landcover6k/intro), which in turn
received support from the Swiss National Science Foundation, the Swiss Academy of Sciences, the US
National Science Foundation, and the Chinese Academy of Sciences. This work is also supported
through an NSERC Discovery Grant to A. Dawson. M.-J. Gaillard received support from the Swedish
Strategic Research Area (SRA) MERGE (ModElling the Regional and Global Earth system;





http://www.merge.lu.se. Data were obtained from the Neotoma Paleoecology Database
 (http://www.neotomadb.org) and its constituent database the North American Pollen Database. The work
 of data contributors, data stewards, and the Neotoma community is gratefully acknowledged. Support for
 Neotoma is from the NSF-Geoinformatics program (1948926). Digitization of basin areas was assisted
 by Jenna Kilsevich, Grace Roper, Claire Rubbelke, Grace Tunski, Mathias Trachsel, and Bailey Zak.





10. References 892

- Abraham, V., Oušková, V., and Kuneš, P.: Present-day vegetation helps quantifying past land 894 cover in selected regions of the Czech Republic, PLoS One, 9, e100117, 2014.
- Alder, J. R. and Hostetler, S. W.: Global climate simulations at 3000-year intervals for the last 21 000 years with the GENMOM coupled atmosphere-ocean model, Clim. Past, 11, 449-471, 896 https://doi.org/10.5194/cp-11-449-2015, 2015.
- 898 Alessandri, A., Catalano, F., De Felice, M., Van den Hurk, B., and Balsamo, G.: Varying snow and vegetation signatures of surface-albedo feedback on the Northern Hemisphere land warming, Environ.
- 900 Res. Lett., 16, 034023, 2021.
- Allison, T. D., Moeller, R. E., and Davis, M. B.: Pollen in laminated sediments provides evidence of mid-902 Holocene forest pathogen outbreak, Ecology, 67, 1101–1105, 1986.
- Alt, M., McWethy, D. B., Everett, R., and Whitlock, C.: Millennial scale climate-fire-vegetation 904 interactions in a mid-elevation mixed coniferous forest, Mission Range, northwestern Montana, USA, Quat. Res., 90, 66-82, 2018.
- 906 Anderson, L. L., Hu, F. S., Nelson, D. M., Petit, R. J., and Paige, K. N.: Ice-age endurance: DNA evidence of a white spruce refugium in Alaska, Proc. Natl. Acad. Sci., 103, 12447-12450, 2006.
- 908 Anderson, P. M. and Brubaker, L. B.: Vegetation history of northcentral Alaska: A mapped summary of late-Quaternary pollen data, Quat. Sci. Rev., 13, 71–92, https://doi.org/10.1016/0277-3791(94)90125-2, 910 1994.
- Anderson, R. S.: Postglacial biogeography of Sierra lodgepole pine (Pinus contorta var. murrayana) in 912 California, Écoscience, 3, 343–351, https://doi.org/10.1080/11956860.1996.11682352, 1996.
- Anderson, R. S. and Carpenter, S. L.: Vegetation change in Yosemite Valley, Yosemite National Park, 914 California, during the protohistoric period, Madroño, 38, 1–13, 1991.
- Anderson, R. S., Davis, R. B., Miller, N. G., and Stuckenrath, Jr., R.: History of late- and post-glacial 916 vegetation and disturbance around Upper South Branch Pond, northern Maine, Can. J. Bot., 64, 1977-1986, 1986.
- 918 Anderson, R. S., Allen, C. D., Toney, J. L., Jass, R. B., and Bair, A. N.: Holocene vegetation and fire regimes in subalpine and mixed conifer forests, southern Rocky Mountains, USA, Int. J. Wildland Fire,
- 920 17, 96–114, 2008.
- Anderson, R. S., Kaufman, D. S., Berg, E., Schiff, C., and Daigle, T.: Holocene biogeography of Tsuga 922 mertensiana and other conifers in the Kenai Mountains and Prince William Sound, south-central Alaska, The Holocene, 27, 485–495, https://doi.org/10.1177/0959683616670217, 2017.
- 924 Anderson, R. S., Berg, E., Williams, C., and Clark, T.: Postglacial vegetation community change over an elevational gradient on the western Kenai Peninsula, Alaska: pollen records from Sunken Island and
- 926 Choquette Lakes, J. Quat. Sci., 34, 309–322, https://doi.org/10.1002/jqs.3102, 2019.





- Azuara, J., Mazier, F., Lebreton, V., Sugita, S., Viovy, N., and Combourieu-Nebout, N.: Extending the applicability of the REVEALS model for pollen-based vegetation reconstructions to coastal lagoons, The Holocene, 29, 1109–1112, 2019.
- 930 Bartlein, P. J., Hostletler, S. W., and Alder, J. R.: Paleoclimate, in: Climate Change in North America, Springer International Publishing, 1–51, 2014.
- Bathiany, S., Claussen, M., Brovkin, V., Raddatz, T., and Gayler, V.: Combined biogeophysical and biogeochemical effects of large-scale forest cover changes in the MPI earth system model,
- 934 Biogeosciences, 7, 1383–1399, 2010.
- Bhiry, N. and Filion, L.: Mid-Holocene hemlock decline in eastern North America linked with
- phytophagous insect activity, Quat. Res., 45, 312–320, 1996.
- Black, B. A., Ruffner, C. M., and Abrams, M. D.: Native American influences on the forest composition of the Allegheny Plateau, northwest Pennsylvania, Can. J. For. Res., 36, 1266–1275, https://doi.org/10.1139/x06-027, 2006.
- 940 Bodmer, H.: Über den windpollen, Nat. Tech., 3, 294–298, 1922.
 - Bonan, G.: Ecological climatology: concepts and applications, 2015.
- Bonan, G. B. and Doney, S. C.: Climate, ecosystems, and planetary futures: The challenge to predict life in Earth system models, Science, 359, eaam8328, 2018.
- Booth, R. K., Brewer, S., Blaauw, M., Minckley, T. A., and Jackson, S. T.: Decomposing the mid Holocene Tsuga decline in eastern North America, Ecology, 93, 1841–1852, https://doi.org/10.1890/11-
- 946 2062.1, 2012.
- Bothe, O., Jungclaus, J. H., Zanchettin, D., and Zorita, E.: Climate of the last millennium: ensemble consistency of simulations and reconstructions, Clim Past, 9, 1089–1110, https://doi.org/10.5194/cp-9-1089-2013, 2013.
- 950 Bradshaw, R. H. W. and Webb, I., T.: Relationships between contemporary pollen and vegetation data from Wisconsin and Michigan, USA, Ecology, 66, 721–737, 1985.
- 952 Briles, C. E., Whitlock, C., Bartlein, P. J., and Higuera, P.: Regional and local controls on postglacial vegetation and fire in the Siskiyou Mountains, northern California, USA, Palaeogeogr. Palaeoclimatol.
- 954 Palaeoecol., 265, 159–169, 2008.
- Broström, A., Nielsen, A. B., Gaillard, M.-J., Hjelle, K., Mazier, F., Binney, H., Bunting, J., Fyfe, R., Meltsov, V., and Poska, A.: Pollen productivity estimates of key European plant taxa for quantitative reconstruction of past vegetation: a review, Veg. Hist. Archaeobotany, 17, 461–478, 2008.
- Brovkin, V., Raddatz, T., Reick, C. H., Claussen, M., and Gayler, V.: Global biogeophysical interactions between forest and climate, Geophys. Res. Lett., 36, 2009.
- 960 Brugam, R. B. and Swain, P.: Diatom indicators of peatland development at Pogonia Bog Pond, Minnesota, USA, The Holocene, 10, 453–464, https://doi.org/10.1191/095968300668251084, 2000.





- 962 Brugger, S. O. and Rhode, D.: Impact of Pleistocene–Holocene climate shifts on vegetation and fire dynamics and its implications for Prearchaic humans in the central Great Basin, USA, J. Quat. Sci., 35,
- 964 987–993, https://doi.org/10.1002/jqs.3248, 2020.
- Calder, W. J. and Shuman, B. N.: Extensive wildfires, climate change, and an abrupt state change in subalpine ribbon forests, Colorado, Ecology, 98, 2585–2600, 2017.
- Chandan, D. and Peltier, W. R.: African Humid Period Precipitation Sustained by Robust Vegetation, Soil, and Lake Feedbacks, Geophys. Res. Lett., 47, e2020GL088728, https://doi.org/10.1029/2020GL088728, 2020.
- Ohaput, M. A. and Gajewski, K.: Relative pollen productivity estimates and changes in Holocene vegetation cover in the deciduous forest of southeastern Quebec, Canada, Botany, 96, 299–317,
- 972 https://doi.org/10.1139/cjb-2017-0193, 2018.
- Chen, J., Zhang, Q., Huang, W., Lu, Z., Zhang, Z., and Chen, F.: Northwestward shift of the northern boundary of the East Asian summer monsoon during the mid-Holocene caused by orbital forcing and vegetation feedbacks, Quat. Sci. Rev., 268, 107136, https://doi.org/10.1016/j.quascirev.2021.107136,
- 976 2021.
- Chen, L. and Dirmeyer, P. A.: Adapting observationally based metrics of biogeophysical feedbacks from land cover/land use change to climate modeling, Environ. Res. Lett., 11, 034002, 2016.
- Chevalier, M., Davis, B. A. S., Heiri, O., Seppä, H., Chase, B. M., Gajewski, K., Lacourse, T., Telford, R. J., Finsinger, W., Guiot, J., Kühl, N., Maezumi, S. Y., Tipton, J. R., Carter, V. A., Brussel, T., Phelps, L. N., Dawson, A., Zanon, M., Vallé, F., Nolan, C., Mauri, A., de Vernal, A., Izumi, K., Holmström, L.,
- 982 Marsicek, J., Goring, S., Sommer, P. S., Chaput, M., and Kupriyanov, D.: Pollen-based climate reconstruction techniques for late Quaternary studies, Earth-Sci. Rev., 210, 103384,
- 984 https://doi.org/10.1016/j.earscirev.2020.103384, 2020.
- Clark, J. S., Hussey, T., and Royall, P. D.: Presettlement analogs for Quaternary fire regimes in eastern North America, J. Paleolimnol., 16, 79–96, 1996.
- Cruz-Silva, E., Harrison, S. P., Marinova, E., and Prentice, I. C.: A new method based on surface-sample pollen data for reconstructing palaeovegetation patterns, J. Biogeogr., 49, 1381–1396, https://doi.org/10.1111/jbi.14448, 2022.
- Owynar, L. C. and Spear, R. W.: Paleovegetation and paleoclimatic changes in the Yukon at 6 ka BP, Géographie Phys. Quat., 49, 29–35, 1995.
- Dallmeyer, A., Kleinen, T., Claussen, M., Weitzel, N., Cao, X., and Herzschuh, U.: The deglacial forest conundrum, Nat. Commun., 13, 6035, https://doi.org/10.1038/s41467-022-33646-6, 2022.
- Dallmeyer, A., Poska, A., Marquer, L., Seim, A., and Gaillard-Lemdahl, M.-J.: The challenge of comparing pollen-based quantitative vegetation reconstructions with outputs from vegetation models—a
- 996 European perspective, Clim. Past Discuss., 2023, 1–50, 2023.
- Dalton, A. S., Margold, M., Stokes, C. R., Tarasov, L., Dyke, A. S., Adams, R. S., Allard, S., Arends, H. 998 E., Atkinson, N., Attig, J. W., Barnett, P. J., Barnett, R. L., Batterson, M., Bernatchez, P., Borns, H. W., Breckenridge, A., Briner, J. P., Brouard, E., Campbell, J. E., Carlson, A. E., Clague, J. J., Curry, B. B.,
- 1000 Daigneault, R.-A., Dubé-Loubert, H., Easterbrook, D. J., Franzi, D. A., Friedrich, H. G., Funder, S.,





- Gauthier, M. S., Gowan, A. S., Harris, K. L., Hétu, B., Hooyer, T. S., Jennings, C. E., Johnson, M. D.,
- 1002 Kehew, A. E., Kelley, S. E., Kerr, D., King, E. L., Kjeldsen, K. K., Knaeble, A. R., Lajeunesse, P., Lakeman, T. R., Lamothe, M., Larson, P., Lavoie, M., Loope, H. M., Lowell, T. V., Lusardi, B. A., Manz,
- L., McMartin, I., Nixon, F. C., Occhietti, S., Parkhill, M. A., Piper, D. J. W., Pronk, A. G., Richard, P. J. H., Ridge, J. C., Ross, M., Roy, M., Seaman, A., Shaw, J., Stea, R. R., Teller, J. T., Thompson, W. B.,
- 1006 Thorleifson, L. H., Utting, D. J., Veillette, J. J., Ward, B. C., Weddle, T. K., and Wright, H. E.: An updated radiocarbon-based ice margin chronology for the last deglaciation of the North American Ice
- 1008 Sheet Complex, Quat. Sci. Rev., 234, 106223, https://doi.org/10.1016/j.quascirev.2020.106223, 2020.
- Davis, M. B.: Pollen evidence of changing land use around the shores of Lake Washington, Northwest Sci., 47, 133–148, 1973.
- Davis, M. B.: Outbreaks of forest pathogens in Quaternary history, in: Proceedings of the Fourth International Palynological Conference, Lucknow, India, 216–227, 1981.
- international Faryhological Conference, Eucknow, India, 210–227, 1701.
- Davis, M. B.: Palynology after Y2K—understanding the source area of pollen in sediments, Annu. Rev. Earth Planet. Sci., 28, 1–18, 2000.
 - Dawson, A., Paciorek, C. J., McLachlan, J. S., Goring, S., Williams, J. W., and Jackson, S. T.:
- Quantifying pollen-vegetation relationships to reconstruct ancient forests using 19th-century forest composition and pollen data, Quat. Sci. Rev., 137, 156–175, 2016.
- Dawson, A., Cao, X., Chaput, M., Hopla, E., Li, F., Edwards, M., Fyfe, R., Gajewski, K., Goring, S., Herzschuh, U., and others: Finding the magnitude of human-induced Northern Hemisphere land-cover
- transformation between 6 and 0.2 ka BP, PAGES Mag, 26, 34–35, 2018.
- Dawson, A., Paciorek, C. J., Goring, S. J., Jackson, S. T., McLachlan, J. S., and Williams, J. W.:
- Quantifying trends and uncertainty in prehistoric forest composition in the upper Midwestern United States, Ecology, 100, e02856, https://doi.org/10.1002/ecy.2856, 2019a.
- Dawson, A., Paciorek, C. J., Goring, S., Jackson, S., McLachlan, J., and Williams, J. W.: Quantifying trends and uncertainty in prehistoric forest composition in the upper Midwestern United States, Ecology,
- 1026 doi: 10.1002/ecy.2856, 2019b.
- Dean, W. E., Bradbury, J. P., Anderson, R. Y., and Barnosky, C. W.: The variability of Holocene climate
- thange: Evidence from varved lake sediments, Science, 226, 1191–1194, https://doi.org/10.1126/science.226.4679.1191, 1984.
- https://doi.org/10.1126/science.226.4679.1191, 1984.
- Delcourt, H. R. and Delcourt, P. A.: Postglacial rise and decline of Ostrya virginiana (Mill) K Koch and Carpinus caroliniana Walt in eastern North-America: Predictable responses of forest species to cyclic
- changes in seasonality of climates, J. Biogeogr., 21, 137–150, 1994.
- Delcourt, P. A., Delcourt, H. R., Cridlebaugh, P. A., and Chapman, J.: Holocene ethnobotanical and paleoecological record of human impact on vegetation in the Little Tennessee River Valley, Tennessee, Quat. Res., 25, 330–349, 1986.
- Deser, C., Lehner, F., Rodgers, K. B., Ault, T., Delworth, T. L., DiNezio, P. N., Fiore, A., Frankignoul, C., Fyfe, J. C., Horton, D. E., Kay, J. E., Knutti, R., Lovenduski, N. S., Marotzke, J., McKinnon, K. A.,
- Minobe, S., Randerson, J., Screen, J. A., Simpson, I. R., and Ting, M.: Insights from Earth system model initial-condition large ensembles and future prospects, Nat. Clim. Change, 10, 277–286,
- 1040 https://doi.org/10.1038/s41558-020-0731-2, 2020.





- Edwards, M. E., Brubaker, L. B., Lozhkin, A. V., and Anderson, P. M.: Structurally novel biomes: a response to past warming in Beringia, Ecology, 86, 1696–1703, 2005.
- Ellis, E. C.: Land use and ecological change: A 12,000-Year History, Annu. Rev. Environ. Resour., 46, 1–33, https://doi.org/10.1146/annurev-environ-012220-010822, 2021.
- Evans, M. N., Tolwinski-Ward, S. E., Thompson, D. M., and Anchukaitis, K. J.: Applications of proxy system modeling in high resolution paleoclimatology, Quat. Sci. Rev., 76, 16–28, http://dx.doi.org/10.1016/j.quascirev.2013.05.024, 2013.
- Faison, E. K., Foster, D. R., Oswald, W. W., Hansen, B. C. S., and Doughty, E.: Early Holocene openlands in southern New England, Ecology, 87, 2537–2547, 2006.
- Finkelstein, S. A., Gajewski, K., and Viau, A. E.: Improved resolution of pollen taxonomy allows better biogeographical interpretation of post-glacial forest development: analyses from the North American
- 1052 Pollen Database, J. Ecol., 94, 415–430, 2006.
- Flantua, S. G. A., Mottl, O., Felde, V. A., Bhatta, K. P., Birks, H. H., Grytnes, J.-A., Seddon, A. W. R.,
- and Birks, H. J. B.: A guide to the processing and standardization of global palaeoecological data for large-scale syntheses using fossil pollen, Glob. Ecol. Biogeogr., n/a, https://doi.org/10.1111/geb.13693,
- 1056 2023.
- Foley, J. A., Kutzbach, J. E., Coe, M. T., and Levis, S.: Feedbacks between climate and boreal forests during the Holocene epoch, Nature, 371, 52–54, 1994.
- Foster, D. R. and Aber, J. D.: Forests in Time: The Environmental Consequences of 1000 Years of Change in New England, Yale University Press, New Haven, CT., 2004.
- Foster, D. R., Oswald, W. W., Faison, E. K., Doughty, E. D., and Hansen, B. C. S.: A climatic driver for abrupt mid-Holocene vegetation dynamics and the hemlock decline in New England, Ecology, 87, 2959–2966, 2006.
- Fréchette, B., Richard, P. J. H., Grondin, P., Lavoie, M., and Larouche, A. C.: Postglacial history of the vegetation and climate of the spruce and fir forests of western Quebec, Mém. Rech. For., 179, 2018.
- Fréchette, B., Richard, P. J. H., Lavoie, M., Grondin, P., and Larouche, A. C.: Histoire postglaciaire de la végétation et du climat des pessières et des sapinières de l'est du Québec et du Labrador méridional,
- 1068 Mém. Rech. For., 186, 170, 2021.
- Fyfe, R., Roberts, N., and Woodbridge, J.: A pollen-based pseudobiomisation approach to anthropogenic land-cover change, The Holocene, 20, 1165–1171, https://doi.org/10.1177/0959683610369509, 2010.
- Gaillard, M., Whitehouse, N., Madella, M., Morrison, K., and von Gunten, L.: Past Land Use and Land Cover., PAGES Mag., 26, 2018.
- Gaillard, M. J. and Group, L. I. S.: LandCover6k: Global anthropogenic land-cover change and its role in past climate, PAGES Mag., 23, 38–39, 2015.
- Gaillard, M.-J., Sugita, S., Mazier, F., Trondman, A.-K., Broström, A., Hickler, T., Kaplan, J. O.,

 Kjellström, E., Kokfelt, U., Kuneš, P., Lemmen, C., Miller, P., Olofsson, J., Poska, A., Rundgren, M.,
 Smith, B., Strandberg, G., Fyfe, R., Nielsen, A. B., Alenius, T., Balakauskas, L., Barnekow, L., Birks, H.





- J. B., Bjune, A., Björkman, L., Giesecke, T., Hjelle, K., Kalnina, L., Kangur, M., van der Knaap, W. O., Koff, T., Lagerås, P., Latalowa, M., Leydet, M., Lechterbeck, J., Lindbladh, M., Odgaard, B., Peglar, S.,
- Segerström, U., von Stedingk, H., and Seppä, H.: Holocene land-cover reconstructions for studies on land cover-climate feedbacks, Clim. Past, 6, 483–499, https://doi.org/10.5194/cp-6-483-2010, 2010.
- Gajewski, K.: Environmental history of the northwestern Québec Treeline, Quat. Sci. Rev., 206, 29–43, https://doi.org/10.1016/j.quascirev.2018.12.025, 2019.
- Gajewski, K., Kriesche, B., Chaput, M. A., Kulik, R., and Schmidt, V.: Human-vegetation interactions during the Holocene in North America, Veg. Hist. Archaeobotany, 28, 635–647,
- 1086 https://doi.org/10.1007/s00334-019-00721-w, 2019.
- Gajewski, K., Grenier, A., and Payette, S.: Climate, fire and vegetation history at treeline east of Hudson Bay, northern Québec, Quat. Sci. Rev., 254, 106794, https://doi.org/10.1016/j.quascirev.2021.106794, 2021.
- Gavin, D. G. and Brubaker, L. B.: Late Pleistocene and Holocene Environmental Change on the Olympic Peninsula, Washington, Springer, 2014.
- Gavin, D. G., Brubaker, L. B., and Greenwald, D. N.: Postglacial climate and fire-mediated vegetation change on the western Olympic Peninsula, Washington (USA), Ecol. Monogr., 83, 471–489,
- 1094 https://doi.org/10.1890/12-1742.1, 2013.
- Gavin, D. G., White, A., Sanborn, P. T., and Hebda, R. J.: Deglacial landforms and Holocene vegetation trajectories in the northern interior cedar-hemlock forests of British Columbia, in: Untangling the Quaternary Period—A Legacy of Stephen C. Porter, vol. 548, edited by: Waitt, R. B., Thackray, G. D.,
- 1098 and Gillespie, A. R., Geological Society of America, 0, https://doi.org/10.1130/2020.2548(05), 2021.
- George, A., Widell, S., Goring, S. J., Roth, R. E., and Williams, J. W.: Range Mapper: An adaptable process for making and using interactive, animated web maps of late-Quaternary open paleoecological data, Open Quat., 9, 15, https://doi.org/10.5334/oq.114, 2023.
- Githumbi, E., Fyfe, R., Gaillard, M.-J., Trondman, A.-K., Mazier, F., Nielsen, A.-B., Poska, A., Sugita, S., Woodbridge, J., Azuara, J., Feurdean, A., Grindean, R., Lebreton, V., Marquer, L., Nebout-
- 1104 Combourieu, N., Stančikaitė, M., Tanţău, I., Tonkov, S., Shumilovskikh, L., and LandClimII data contributors: European pollen-based REVEALS land-cover reconstructions for the Holocene:
- 1106 methodology, mapping and potentials, Earth Syst Sci Data, 14, 1581–1619, https://doi.org/10.5194/essd-14-1581-2022, 2022a.
- 1108 Githumbi, E., Pirzamanbein, B., Lindström, J., Poska, A., Fyfe, R., Mazier, F., Nielsen, A. B., Sugita, S., Trondman, A.-K., Woodbridge, J., and Gaillard, M.-J.: Pollen-Based Maps of Past Regional Vegetation
- 1110 Cover in Europe Over 12 Millennia—Evaluation and Potential, Front. Ecol. Evol., 10, https://doi.org/10.3389/fevo.2022.795794, 2022b.
- 1112 Githumbi, E., Pirzamanbein, B., Lindström, J., Poska, A., Fyfe, R., Mazier, F., Nielsen, A. B., Sugita, S., Trondman, A.-K., Woodbridge, J., and others: Pollen-Based Maps of Past Regional Vegetation Cover in
- 1114 Europe Over 12 Millennia—Evaluation and Potential, Front. Ecol. Evol., 10, 795794, 2022c.
- Giuliano, C. and Lacourse, T.: Holocene fire regimes, fire-related plant functional types, and climate in south-coastal British Columbia forests, Ecosphere, 14, e4416, https://doi.org/10.1002/ecs2.4416, 2023.





- Goring, S.: neotoma_lakes, 2021.
- 1118 Grimm, E. C., Keltner, J., Cheddadi, R., Hicks, S., Lézine, A.-M., Berrio, J. C., and Williams, J. W.: Pollen databases and their application, in: Encyclopedia of Quaternary Science, edited by: Elias, S. A. and
- 1120 Mock, C. J., Elsevier, 831–838, 2013.
- Gugger, P. F. and Sugita, S.: Glacial populations and postglacial migration of Douglas-fir based on fossil pollen and macrofossil evidence, Quat. Sci. Rev., 29, 2052–2070, 2010.
- Haas, J. N. and McAndrews, J. H.: The summer drought related hemlock (Tsuga canadensis) decline in eastern North America 5,700 to 5,100 years ago, Symposium on Sustainable Management of Hemlock Ecosystems in Eastern North America, 1999.
- Hansen, B. C. S. and Engstrom, D. R.: Vegetation History of Pleasant Island, Southeastern Alaska, since 13,000 yr B.P., Quat. Res., 46, 161–175, https://doi.org/10.1006/qres.1996.0056, 1996.
- Harrison, S. P., Gaillard, M. J., Stocker, B. D., Vander Linden, M., Klein Goldewijk, K., Boles, O., Braconnot, P., Dawson, A., Fluet-Chouinard, E., Kaplan, J. O., Kastner, T., Pausata, F. S. R., Robinson,
- E., Whitehouse, N. J., Madella, M., and Morrison, K. D.: Development and testing scenarios for implementing land use and land cover changes during the Holocene in Earth system model experiments,
- 1132 Geosci Model Dev, 13, 805–824, https://doi.org/10.5194/gmd-13-805-2020, 2020.
- Hayashi, R., Sasaki, N., Takahara, H., Sugita, S., and Saito, H.: Estimation of absolute pollen productivity based on the flower counting approach: A review, Quat. Int., 641, 122–137, 2022.
- Hellman, S., Gaillard, M.-J., Broström, A., and Sugita, S.: The REVEALS model, a new tool to estimate past regional plant abundance from pollen data in large lakes: validation in southern Sweden, J. Quat. Sci. Publ. Quat. Res. Assoc., 23, 21–42, 2008a.
- Hellman, S. E., Gaillard, M., Broström, A., and Sugita, S.: Effects of the sampling design and selection of parameter values on pollen-based quantitative reconstructions of regional vegetation: a case study in
- 1140 southern Sweden using the REVEALS model, Veg. Hist. Archaeobotany, 17, 445–459, 2008b.
- Herzschuh, U.: Legacy of the Last Glacial on the present-day distribution of deciduous versus evergreen boreal forests, Glob. Ecol. Biogeogr., 29, 198–206, https://doi.org/10.1111/geb.13018, 2020.
- Herzschuh, U., Böhmer, T., Li, C., Chevalier, M., Hébert, R., Dallmeyer, A., Cao, X., Bigelow, N. H.,
 Nazarova, L., and Novenko, E. Y.: LegacyClimate 1.0: a dataset of pollen-based climate reconstructions from 2594 Northern Hemisphere sites covering the last 30 kyr and beyond, Earth Syst. Sci. Data, 15,
- 1146 2235–2258, 2023.
- Hoevers, R., Broothaerts, N., and Verstraeten, G.: The potential of REVEALS-based vegetation reconstructions using pollen records from alluvial floodplains, Veg. Hist. Archaeobotany, 31, 525–540, 2022.
- Hogg, D.: High-Resolution Analysis of Snow Albedo Interactions in the Arctic, University of Waterloo, 2022.
- Hollinger, D. Y., Ollinger, S. V., Richardson, A. D., Meyers, T. P., Dail, D. B., Martin, M. E., Scott, N. A., Arkebauer, T. J., Baldocchi, D. D., and Clark, K. L.: Albedo estimates for land surface models and





- support for a new paradigm based on foliage nitrogen concentration, Glob. Change Biol., 16, 696–710, 2010.
- Huybers, P.: Early Pleistocene Glacial Cycles and the Integrated Summer Insolation Forcing, Science, 313, 508–511, https://doi.org/doi:10.1126/science.1125249, 2006.
- Iglesias, V. and Whitlock, C.: If the trees burn, is the forest lost? Past dynamics in temperate forests help inform management strategies, Philos. Trans. R. Soc. B, 375, 20190115, 2020.
- Iglesias, V., Whitlock, C., Krause, T. R., and Baker, R. G.: Past vegetation dynamics in the Yellowstone region highlight the vulnerability of mountain systems to climate change, J. Biogeogr., 45, 1768–1780,
- **1162** 2018.
- Ireland, A. W. and Booth, R. K.: Hydroclimatic variability drives episodic expansion of a floating peat mat in a North American kettlehole basin, Ecology, 92, 11–18, https://doi.org/10.1890/10-0770.1, 2010.
- Islebe, G. A., Hooghiemstra, H., Brenner, M., Curtis, J. H., and Hodell, D. A.: A Holocene vegetation history from lowland Guatemala, The Holocene, 6, 265–271, https://doi.org/10.1177/095968369600600302, 1996.
- Jackson, S. T.: Pollen source area and representation in small lakes of the northeastern United States, Rev. Palaeobot. Palynol., 63, 53–76, 1990.
- Jackson, S. T. and Lyford, M. E.: Pollen dispersal models in Quaternary plant ecology: assumptions, parameters, and prescriptions, Bot. Rev., 65, 39–75, 1999a.
- Jackson, S. T. and Lyford, M. E.: Pollen dispersal models in Quaternary plant ecology: Assumptions, parameters, and prescriptions, Bot. Rev., 65, 39–75, 1999b.
- Jackson, S. T. and Whitehead, D. R.: Holocene vegetation patterns in the Adirondack Mountains, Ecology, 72, 641–654, 1991.
- Jackson, S. T., Overpeck, J. T., Webb, I., T., Keattch, S. E., and Anderson, K. H.: Mapped plant-macrofossil and pollen records of late Quaternary vegetation change in eastern North America, Quat. Sci.
- 1178 Rev., 16, 1–70, 1997.
- Jackson, S. T., Betancourt, J. L., Booth, R. K., and Gray, S. T.: Ecology and the ratchet of events: Climate variability, niche dimensions, and species distributions, Proc. Natl. Acad. Sci., 106, 19685–19692, 2009.
 - Jensen, A. M., Fastovich, D., Watson, B. I., Gill, J. L., Jackson, S. T., Russell, J. M., Bevington, J.,
- Hayes, K., Lininger, K., Rubbelke, C., Schellinger, G. C., and Williams, J. W.: More than one way to kill a spruce forest: The role of fire and climate in the late-glacial termination of spruce woodlands across the
- southern Great Lakes, J. Ecol., 109, 459–477, https://doi.org/10.1111/1365-2745.13517, 2021.
- Kaplan, J. O., Krumhardt, K. M., and Zimmermann, N.: The prehistoric and preindustrial deforestation of Europe, Quat. Sci. Rev., 28, 3016–3034, https://doi.org/Doi 10.1016/J.Quascirev.2009.09.028, 2009.
- Kaplan, J. O., Krumhardt, K. M., Gaillard, M.-J., Sugita, S., Trondman, A.-K., Fyfe, R., Marquer, L.,
 Mazier, F., and Nielsen, A. B.: Constraining the deforestation history of Europe: Evaluation of historical land use scenarios with pollen-based land cover reconstructions, Land, 6, 91, 2017.





- Kaufman, D. S. and Broadman, E.: Revisiting the Holocene global temperature conundrum, Nature, 614, 425–435, https://doi.org/10.1038/s41586-022-05536-w, 2023.
- 1192 Kelly, R., Chipman, M. L., Higuera, P. E., Stefanova, I., Brubaker, L. B., and Hu, F. S.: Recent burning of boreal forests exceeds fire regime limits of the past 10,000 years, Proc. Natl. Acad. Sci., 110, 13055–
- 1194 13060, https://doi.org/10.1073/pnas.1305069110, 2013.
- Klein Goldewijk, K., Beusen, A., and Janssen, P.: Long-term dynamic modeling of global population and built-up area in a spatially explicit way: HYDE 3.1, The Holocene, 20, 565–573, https://doi.org/10.1177/0959683609356587, 2010.
- Klein Goldewijk, K., Beusen, A., van Drecht, G., and de Vos, M.: The HYDE 3.1 spatially explicit database of human-induced global land-use change over the past 12,000 years, Glob. Ecol. Biogeogr., 20,
- 1200 73–86, https://doi.org/10.1111/j.1466-8238.2010.00587.x, 2011.
 - Knight, C. A., Anderson, L., Bunting, M. J., Champagne, M., Clayburn, R. M., Crawford, J. N.,
- 1202 Klimaszewski-Patterson, A., Knapp, E. E., Lake, F. K., Mensing, S. A., Wahl, D., Wanket, J., Watts-Tobin, A., Potts, M. D., and Battles, J. J.: Land management explains major trends in forest structure and
- 1204 composition over the last millennium in California's Klamath Mountains, Proc. Natl. Acad. Sci., 119, e2116264119, https://doi.org/10.1073/pnas.2116264119, 2022.
- Kuparinen, A., Markkanen, T., Riikonen, H., and Vesala, T.: Modeling air-mediated dispersal of spores, pollen and seeds in forested areas, Ecol. Model., 208, 177–188, 2007.
- 1208 Lacourse, T.: Environmental change controls postglacial forest dynamics through interspecific differences in life-history traits, Ecology, 90, 2149–2160, 2009.
- 1210 Lacourse, T. and Adeleye, M. A.: Climate and species traits drive changes in Holocene forest composition along an elevation gradient in Pacific Canada, Front. Ecol. Evol., 10,
- 1212 https://doi.org/10.3389/fevo.2022.838545, 2022.
- Lacourse, T., Mathewes, R. W., and Hebda, R. J.: Paleoecological analyses of lake sediments reveal prehistoric human impact on forests at Anthony Island UNESCO World Heritage Site, Queen Charlotte Islands (Haida Gwaii), Canada, Quat. Res., 68, 177–183, http://dx.doi.org/10.1016/j.yqres.2007.04.005,
- 1216 2007.
- Lacourse, T., Delepine, J. M., Hoffman, E. H., and Mathewes, R. W.: A 14,000 year vegetation history of a hypermaritime island on the outer Pacific coast of Canada based on fossil pollen, spores and conifer stomata, Quat. Res., 78, 572–582, http://dx.doi.org/10.1016/j.yqres.2012.08.008, 2012.
- Leopold, E. B. and Boyd, R.: An ecological history of old prairie areas, southwestern Washington, in: Indians, Fire and the Land, edited by: Boyd, R., Oregon State University Press, Corvallis OR, 139–166,
- 1222 1999.
 - Lewis, S. L. and Maslin, M. A.: Defining the Anthropocene, Nature, 519, 171–180,
- 1224 https://doi.org/10.1038/nature14258, 2015.
- Li, F., Gaillard, M.-J., Cao, X., Herzschuh, U., Sugita, S., Tarasov, P. E., Wagner, M., Xu, Q., Ni, J., and
- Wang, W.: Towards quantification of Holocene anthropogenic land-cover change in temperate China: A review in the light of pollen-based REVEALS reconstructions of regional plant cover, Earth-Sci. Rev.,
- 1228 203, 103119, 2020.





- Li, F., Gaillard, M.-J., Xie, S., Huang, K., Cui, Q., Fyfe, R., Marquer, L., and Sugita, S.: Evaluation of 1230 relative pollen productivities in temperate China for reliable pollen-based quantitative reconstructions of Holocene plant cover, Front. Plant Sci., 14, 2023a.
- 1232 Li, F., Gaillard, M.-J., Cao, X., Herzschuh, U., Sugita, S., Ni, J., Zhao, Y., An, C., Huang, X., Li, Y., Liu, H., Sun, A., and Yao, Y.: Gridded pollen-based Holocene regional plant cover in temperate and northern
- 1234 subtropical China suitable for climate modelling, Earth Syst Sci Data, 15, 95–112, https://doi.org/10.5194/essd-15-95-2023, 2023b.
- 1236 Liefert, D. T. and Shuman, B. N.: Pervasive desiccation of North American lakes during the late Ouaternary, Geophys. Res. Lett., 47, e2019GL086412, https://doi.org/10.1029/2019GL086412, 2020.
- 1238 Lindgren, F., Rue, H., and Lindström, J.: An explicit link between Gaussian fields and Gaussian Markov random fields: the stochastic partial differential equation approach, J. R. Stat. Soc. Ser. B Stat. Methodol.,
- 1240 73, 423–498, 2011.
- Liu, Y., Ogle, K., Lichstein, J. W., and Jackson, S. T.: Estimation of pollen productivity and dispersal: 1242 How pollen assemblages in small lakes represent vegetation, Ecol. Monogr., 92, e1513,
- https://doi.org/10.1002/ecm.1513, 2022.
- 1244 Liu, Z., Zhu, J., Rosenthal, Y., Zhang, X., Otto-Bliesner, B. L., Timmermann, A., Smith, R. S., Lohmann, G., Zheng, W., and Elison Timm, O.: The Holocene temperature conundrum, Proc. Natl. Acad. Sci., 111,
- 1246 E3501–E3505, https://doi.org/10.1073/pnas.1407229111, 2014.
- Long, C. J., Whitlock, C., Bartlein, P. J., and Millspaugh, S. H.: A 9000-year fire history from the Oregon
- 1248 Coast Range, based on a high-resolution charcoal study, Can. J. For. Res., 28, 774-787, 1998.
- Long, C. J., Whitlock, C., and Bartlein, P. J.: Holocene vegetation and fire history of the Coast Range,
- 1250 western Oregon, USA, The Holocene, 17, 917-926, https://doi.org/10.1177/0959683607082408, 2007.
- Loranty, M. M., Berner, L. T., Goetz, S. J., Jin, Y., and Randerson, J. T.: Vegetation controls on northern 1252 high latitude snow-albedo feedback: observations and CMIP 5 model simulations, Glob. Change Biol., 20, 594-606, 2014.
- 1254 MacDonald, G. M.: Postglacial palaeoecology of the subalpine forest-grassland ecotone of southwestern Alberta: new insights on vegetation and climate change in the Canadian Rocky Mountains and adjacent
- 1256 foothills, Palaeogeogr. Palaeoclimatol. Palaeoecol., 73, 155-173, 1989.
- MacDonald, G. M. and Cwynar, L. C.: Post-glacial population growth rates of Pinus contorta ssp. latifolia
- 1258 in western Canada, J. Ecol., 79, 417–429, https://doi.org/10.2307/2260723, 1991.
- Marcott, S. A., Shakun, J. D., Clark, P. U., and Mix, A. C.: A reconstruction of regional and global 1260 temperature for the past 11,300 years, Science, 339, 1198–1201, 2013.
- Marlon, J. R., Bartlein, P. J., Gavin, D. G., Long, C. J., Anderson, R. S., Briles, C. E., Brown, K. J.,
- 1262 Colombaroli, D., Hallett, D. J., and Power, M. J.: Long-term perspective on wildfires in the western USA, Proc. Natl. Acad. Sci., 109, E535-E543, 2012.
- 1264 Marsicek, J., Shuman, B. N., Bartlein, P. J., Shafer, S. L., and Brewer, S.: Reconciling divergent trends and millennial variations in Holocene temperatures, Nature, 554, 92, https://doi.org/10.1038/nature25464
- 1266 https://www.nature.com/articles/nature25464#supplementary-information, 2018.





- McAndrews, J. H. and Turton, C. L.: Canada geese dispersed cultigen pollen grains from prehistoric
- 1268 Iroquoian fields to Crawford Lake, Ontario, Canada, Palynology, 31, 9–18, https://doi.org/10.2113/gspalynol.31.1.9, 2007.
- 1270 McMichael, C. N. H.: Ecological legacies of past human activities in Amazonian forests, New Phytol., n/a, https://doi.org/10.1111/nph.16888, 2020.
- Mensing, S., Smith, J., Burkle Norman, K., and Allan, M.: Extended drought in the Great Basin of western North America in the last two millennia reconstructed from pollen records, 22nd Pac. Clim.
- 1274 Workshop, 188, 79–89, https://doi.org/10.1016/j.quaint.2007.06.009, 2008.
- Minckley, T. A., Whitlock, C., and Bartlein, P. J.: Vegetation, fire, and climate history of the
- 1276 northwestern Great Basin during the last 14,000 years, Quat. Sci. Rev., 26, 2167–2184, https://doi.org/10.1016/j.quascirev.2007.04.009, 2007.
- 1278 Mottl, O., Flantua, S. G. A., Bhatta, K. P., Felde, V. A., Giesecke, T., Goring, S., Grimm, E. C., Haberle, S., Hooghiemstra, H., Ivory, S., Kuneš, P., Wolters, S., Seddon, A. W. R., and Williams, J. W.: Global
- acceleration in rates of vegetation change over the last 18,000 years, Science, 321, 860–864, 2021.
- Munoz, S. E. and Gajewski, K.: Distinguishing prehistoric human influence on late-Holocene forests in
- 1282 southern Ontario, Canada, The Holocene, 20, 967–981, https://doi.org/10.1177/0959683610362815, 2010.
- Munoz, S. E., Schroeder, S., Fike, D. A., and Williams, J. W.: A record of sustained prehistoric and historic land use from the Cahokia region, Illinois, USA, Geology, 42, 499–502,
- 1286 https://doi.org/10.1130/G35541.1, 2014.
- Napier, J. D. and Chipman, M. L.: Emerging palaeoecological frameworks for elucidating plant dynamics in response to fire and other disturbance, Glob. Ecol. Biogeogr., n/a, https://doi.org/10.1111/geb.13416, 2021.
- 1290 Natural Resources Canada: National Hydro Network, 2022.
- Nelson, D. M., Hu, F. S., Grimm, E. C., Curry, B. B., and Slate, J. E.: The influence of aridity and fire on Holocene prairie communities in the eastern Prairie Peninsula, Ecology, 87, 2523–2536, 2006.
- Niklas, K. J.: The motion of windborne pollen grains around conifer ovulate cones: implications on wind pollination, Am. J. Bot., 71, 356–374, 1984.
- Oswald, W. W. and Foster, D. R.: Middle-Holocene dynamics of Tsuga canadensis (eastern hemlock) in northern New England, USA, The Holocene, 22, 71–78, https://doi.org/10.1177/0959683611409774, 2012.
- 1298 Oswald, W. W., Doughty, E. D., Foster, D. R., Shuman, B. N., and Wagner, D. L.: Evaluating the role of insects in the middle-Holocene Tsuga decline, J. Torrey Bot. Soc., 144, 35–39, 2017.
- Oswald, W. W., Foster, D. R., Shuman, B. N., Chilton, E. S., Doucette, D. L., and Duranleau, D. L.: Conservation implications of limited Native American impacts in pre-contact New England, Nat. Sustain.,
- 1302 3, 241–246, https://doi.org/10.1038/s41893-019-0466-0, 2020.





- Otto, J., Raddatz, T., and Claussen, M.: Strength of forest-albedo feedback in mid-Holocene climate simulations, Clim. Past, 7, 1027–1039, 2011.
 - Paciorek, C. J., Goring, S. J., Thurman, A., Cogbill, C. V., Williams, J. W., Mladenoff, D. J., Peters, J. A.,
- 2hu, J., and McLachlan, J. S.: Statistically-estimated tree composition for the northeastern United States at the time of Euro-American settlement, PLoS One, 11, e0150087,
- 1308 http://dx.doi.org/10.1371/journal.pone.0150087, 2016.
- Parnell, A. C., Haslett, J., Allen, J. R., Buck, C. E., and Huntley, B.: A flexible approach to assessing synchroneity of past events using Bayesian reconstructions of sedimentation history, Quat. Sci. Rev., 27, 1872–1885, 2008.
- Payette, S.: A paleo-perspective on ecosystem collapse in boreal North America, edited by: Canadell, J. G. and Jackson, R. B., Ecosyst. Collapse Clim. Change, 101–129, https://doi.org/10.1007/978-3-030-
- **1314** 71330-0 5, 2021.
- Payette, S., Filion, L., and Delwaide, A.: Spatially explicit fire-climate history of the boreal forest-tundra (eastern Canada) over the last 2000 years, Philos. Trans. Biol. Sci., 363, 2301–2316, 2008.
- Payette, S., Couillard, P.-L., Frégeau, M., Laflamme, J., and Lavoie, M.: The velocity of postglacial migration of fire-adapted boreal tree species in eastern North America, Proc. Natl. Acad. Sci., 119, e2210496119, https://doi.org/10.1073/pnas.2210496119, 2022.
- Peros, M. C., Gajewski, K., and Viau, A. E.: Continental-scale tree population response to rapid climate change, competition and disturbance, Glob. Ecol. Biogeogr., 17, 658–669, 2008.
- Peros, M. C., Munoz, S. E., Gajewski, K., and Viau, A. E.: Prehistoric demography of North America inferred from radiocarbon data, J. Archaeol. Sci., 37, 656–664, 2010.
- Perrotti, A. G., Ramiadantsoa, T., O'Keefe, J., and Nuñez Otaño, N.: Uncertainty in coprophilous fungal spore concentration estimates, Front. Ecol. Evol., 10, 2022.
- 1326 Pirzamanbein, B., Lindström, J., Poska, A., Sugita, S., Trondman, A.-K., Fyfe, R., Mazier, F., Nielsen, A. B., Kaplan, J. O., Bjune, A., Birks, H. J. B., Giesecke, T., Kangur, M., Latałowa, M., Marquer, L., Smith,
- B., and Gaillard, M.-J.: Creating spatially continuous maps of past land cover from point estimates: A new statistical approach applied to pollen data, Ecol. Complex., 20, 127–141,
- 1330 https://doi.org/10.1016/j.ecocom.2014.09.005, 2014.
- Pirzamanbein, B., Lindström, J., Poska, A., and Gaillard, M.-J.: Modelling spatial compositional data:
- 1332 Reconstructions of past land cover and uncertainties, Spat. Stat., 24, 14–31, 2018a.
- Pirzamanbein, B., Lindström, J., Poska, A., and Gaillard, M. J.: Modelling spatial compositional data: Reconstructions of past land cover and uncertainties, Spat. Stat., 24, 14–31, 2018b.
- Pirzamanbein, B., Poska, A., and Lindström, J.: Bayesian reconstruction of past land cover from pollen data: Model robustness and sensitivity to auxiliary variables, Earth Space Sci., 7, e2018EA00057, 2020.
- Pongratz, J., Reick, C. H., Raddatz, T., and Claussen, M.: Biogeophysical versus biogeochemical climate response to historical anthropogenic land cover change, Geophys. Res. Lett., 37, L08702, https://doi.org/10.1029/2010GL043010, 2010.





- Prentice, I. C.: Pollen representation, source area, and basin size: toward a unified theory of pollen analysis, Quat. Res., 23, 76–86, 1985.
- Prentice, I. C., Jolly, D., and BIOME 6000 participants: Mid-Holocene and glacial-maximum vegetation geography of the northern continents and Africa, J. Biogeogr., 27, 507–519, 2000.
- Prentice, I. C., Harrison, S. P., and Bartlein, P. J.: Global vegetation and terrestrial carbon cycle changes after the last ice age, New Phytol., 189, 988–998, 2011.
- Rangel, T. F. L. V. B., Diniz-Filho, J. A. F., and Araújo, M. B.: BIOENSEMBLES 1.0, Software for computer intensive ensemble forecasting of species distributions under climate change, 2009.
- Reimer, P. J., Austin, W. E., Bard, E., Bayliss, A., Blackwell, P. G., Ramsey, C. B., Butzin, M., Cheng, H., Edwards, R. L., and Friedrich, M.: The IntCal20 Northern Hemisphere radiocarbon age calibration
- 1350 curve (0–55 cal kBP), Radiocarbon, 62, 725–757, 2020.
- Richard, P., Fréchette, B., Grondin, P., and Lavoie, M.: Histoire postglaciaire de la végétation de la forêt boréale du Québec et du Labrador, Nat. Can., 144, 63–76, https://doi.org/10.7202/1070086ar, 2020.
- Roberts, N., Fyfe, R. M., Woodbridge, J., Gaillard, M. J., Davis, B. A. S., Kaplan, J. O., Marquer, L.,
 Mazier, F., Nielsen, A. B., Sugita, S., Trondman, A. K., and Leydet, M.: Europe's lost forests: a pollen-based synthesis for the last 11,000 years, Sci. Rep., 8, 716, https://doi.org/10.1038/s41598-017-18646-7,
- 1356 2018
- Rogelj, J., Popp, A., Calvin, K. V., Luderer, G., Emmerling, J., Gernaat, D., Fujimori, S., Strefler, J.,
- Hasegawa, T., Marangoni, G., Krey, V., Kriegler, E., Riahi, K., van Vuuren, D. P., Doelman, J., Drouet, L., Edmonds, J., Fricko, O., Harmsen, M., Havlík, P., Humpenöder, F., Stehfest, E., and Tavoni, M.:
- Scenarios towards limiting global mean temperature increase below 1.5 °C, Nat. Clim. Change, 8, 325–332, https://doi.org/10.1038/s41558-018-0091-3, 2018.
- 1362 Roos, C. I.: Scale in the study of Indigenous burning, Nat. Sustain., https://doi.org/10.1038/s41893-020-0579-5, 2020.
- Roos, C. I., Zedeño, M. N., Hollenback, K. L., and Erlick, M. M. H.: Indigenous impacts on North American Great Plains fire regimes of the past millennium, Proc. Natl. Acad. Sci., 115, 8143–8148,
- 1366 https://doi.org/10.1073/pnas.1805259115, 2018.
- Rosenberg, S. M., Walker, I. R., and Mathewes, R. W.: Postglacial spread of hemlock (Tsuga) and vegetation history in Mount Revelstoke National Park, British Columbia, Canada, Can. J. Bot., 81, 139–151, 2003.
- Ruddiman, W. F.: The anthropogenic greenhouse era began thousands of years ago, Clim. Change, 61, 261–293, 2003.
- 1372 Ruddiman, W. F.: The Anthropocene, Annu. Rev. Earth Planet. Sci., 41, 4.1-4.24, 2013.
- Serge, M.-A., Mazier, F., Fyfe, R., Gaillard, M.-J., Klein, T., Lagnoux, A., Galop, D., Githumbi, E.,
 Mindrescu, M., and Nielsen, A. B.: Testing the effect of relative pollen productivity on the REVEALS model: a validated reconstruction of Europe-wide holocene vegetation, Land, 12, 986, 2023.





- 1376 Shuman, B., Webb, T., III, Bartlein, P., and Williams, J. W.: The anatomy of a climatic oscillation: vegetation change in eastern North America during the Younger Dryas chronozone, Quat. Sci. Rev., 21,
- **1378** 1777–1791, 2002.
- Shuman, B. N. and Marsicek, J.: The structure of Holocene climate change in mid-latitude North
- 1380 America, Quat. Sci. Rev., 141, 38–51, 2016.
- Shuman, B. N., Newby, P. C., Huang, Y., and Webb, I., T.: Evidence for the close climatic control of
- New England vegetation history, Ecology, 85, 1297–1310, 2004.
- Shuman, B. N., Stefanescu, I. C., Grigg, L. D., Foster, D. R., and Oswald, W. W.: A millennial-scale oscillation in latitudinal temperature gradients along the western North Atlantic during the mid-Holocene, Geophys. Res. Lett., 50, e2022GL102556, https://doi.org/10.1029/2022GL102556, 2023.
- Snitker, G., Roos, C. I., Sullivan, A. P., Maezumi, S. Y., Bird, D. W., Coughlan, M. R., Derr, K. M., Gassaway, L., Klimaszewski-Patterson, A., and Loehman, R. A.: A collaborative agenda for archaeology
- 1388 and fire science, Nat. Ecol. Evol., https://doi.org/10.1038/s41559-022-01759-2, 2022.
- Spear, R. W., Davis, M. B., and Shane, L. C. K.: Late Quaternary history of low- and mid-elevation vegetation in the White Mountains of New Hampshire, Ecol. Monogr., 64, 85–109, 1994.
- Stegner, M. A. and Spanbauer, T. L.: North American pollen records provide evidence for macroscale ecological changes in the Anthropocene, Proc. Natl. Acad. Sci., 120, e2306815120, https://doi.org/10.1073/pnas.2306815120, 2023.
- Stephens, L., Fuller, D., Boivin, N., Rick, T., Gauthier, N., Kay, A., Marwick, B., Armstrong, C. G., Barton, C. M., Denham, T., Douglass, K., Driver, J., Janz, L., Roberts, P., Rogers, J. D., Thakar, H.,
- Altaweel, M., Johnson, A. L., Sampietro Vattuone, M. M., Aldenderfer, M., Archila, S., Artioli, G., Bale, M. T., Beach, T., Borrell, F., Braje, T., Buckland, P. I., Jiménez Cano, N. G., Capriles, J. M., Diez
- Castillo, A., Çilingiroğlu, Ç., Negus Cleary, M., Conolly, J., Coutros, P. R., Covey, R. A., Cremaschi, M., Crowther, A., Der, L., di Lernia, S., Doershuk, J. F., Doolittle, W. E., Edwards, K. J., Erlandson, J. M.,
- Evans, D., Fairbairn, A., Faulkner, P., Feinman, G., Fernandes, R., Fitzpatrick, S. M., Fyfe, R., Garcea, E., Goldstein, S., Goodman, R. C., Dalpoim Guedes, J., Herrmann, J., Hiscock, P., Hommel, P.,
- Horsburgh, K. A., Hritz, C., Ives, J. W., Junno, A., Kahn, J. G., Kaufman, B., Kearns, C., Kidder, T. R., Lanoë, F., Lawrence, D., Lee, G.-A., Levin, M. J., Lindskoug, H. B., López-Sáez, J. A., Macrae, S.,
- Marchant, R., Marston, J. M., McClure, S., McCoy, M. D., Miller, A. V., Morrison, M., Motuzaite Matuzeviciute, G., Müller, J., Nayak, A., Noerwidi, S., Peres, T. M., Peterson, C. E., Proctor, L., Randall,
- 1406 A. R., Renette, S., Robbins Schug, G., Ryzewski, K., Saini, R., Scheinsohn, V., Schmidt, P., Sebillaud, P., Seitsonen, O., Simpson, I. A., Sołtysiak, A., Speakman, R. J., Spengler, R. N., Steffen, M. L., et al.:
- Archaeological assessment reveals Earth's early transformation through land use, Science, 365, 897–902, https://doi.org/10.1126/science.aax1192, 2019.
- Strandberg, G., Kjellström, E., Poska, A., Wagner, S., Gaillard, M. J., Trondman, A. K., Mauri, A., Davis, B. A. S., Kaplan, J. O., Birks, H. J. B., Bjune, A. E., Fyfe, R., Giesecke, T., Kalnina, L., Kangur, M., van
- der Knaap, W. O., Kokfelt, U., Kuneš, P., Lata, I owa, M., Marquer, L., Mazier, F., Nielsen, A. B., Smith, B., Seppä, H., and Sugita, S.: Regional climate model simulations for Europe at 6 and 0.2 k BP:
- sensitivity to changes in anthropogenic deforestation, Clim Past, 10, 661–680, https://doi.org/10.5194/cp-10-661-2014, 2014.
- 1416 Strandberg, G., Lindström, J., Poska, A., Zhang, Q., Fyfe, R., Githumbi, E., Kjellström, E., Mazier, F., Nielsen, A. B., Sugita, S., Trondman, A.-K., Woodbridge, J., and Gaillard, M.-J.: Mid-Holocene





- European climate revisited: New high-resolution regional climate model simulations using pollen-based land-cover, Quat. Sci. Rev., 281, 107431, https://doi.org/10.1016/j.quascirev.2022.107431, 2022a.
- 1420 Strandberg, G., Lindström, J., Poska, A., Zhang, Q., Fyfe, R., Githumbi, E., Kjellström, E., Mazier, F., Nielsen, A. B., Sugita, S., Trondman, A.-K., Woodbridge, J., and Gaillard, M.-J.: Mid-Holocene
- European climate revisited: New high-resolution regional climate model simulations using pollen-based land-cover, Quat. Sci. Rev., 281, 107431, https://doi.org/10.1016/j.quascirev.2022.107431, 2022b.
- Sugita, S.: Theory of quantitative reconstruction of vegetation I: pollen from large sites REVEALS regional vegetation composition, The Holocene, 17, 229–241, 2007a.
- Sugita, S.: Theory of quantitative reconstruction of vegetation I: pollen from large sites REVEALS regional vegetation composition., The Holocene, 17, 229–241, 2007b.
- Sugita, S.: Theory of quantitative reconstruction of vegetation II: all you need is LOVE, The Holocene, 17, 243–257, 2007c.
- Sugita, S., Parshall, T., Calcote, R., and Walker, K.: Testing the Landscape Reconstruction Algorithm for spatially explicit reconstruction of vegetation in northern Michigan and Wisconsin, Quat. Res., 74, 289–
- 1432 300, 2010.
 - Sutton, O. G.: 1953: Micrometeorology. New York: McGraw-Hill, 1953.
- TEMPO (Testing Earth System Models with Paleo-Observations): Potential role of vegetation feedback in the climate sensitivity of high-latitude regions: A case study at 6000 years B.P., Glob. Biogeochem.
- 1436 Cycles, 10, 727–736, 1996.
- Theuerkauf, M. and Couwenberg: ROPES reveals past land cover and PPEs From single pollen records,
- 1438 Front. Earth Sci., 6, 2018.
 - Theuerkauf, M., Kuparinen, A., and Joosten, H.: Pollen productivity estimates strongly depend on
- 1440 assumed pollen dispersal, The Holocene, DOI: 10.1177/0959683612450194, 2012.
- Theuerkauf, M., Couwenberg, J., Kuparinen, A., and Liebscher, V.: A matter of dispersal: REVEALSinR introduces state-of-the-art dispersal models to quantitative vegetation reconstruction, Veg. Hist. Archaeobotany, 25, 541–553, 2016.
- Thompson, A. J., Zhu, J., Poulsen, C. J., Tierney, J. E., and Skinner, C. B.: Northern Hemisphere vegetation change drives a Holocene thermal maximum, Sci. Adv., 8, eabj6535,
- 1446 https://doi.org/10.1126/sciadv.abj6535, 2022.
- Thompson, J. R., Carpenter, D. N., Cogbill, C. V., and Foster, D. R.: Four centuries of change in northeastern United States forests, PLoS One, 8, e72540, https://doi.org/10.1371/journal.pone.0072540, 2013.
- 1450 Thompson, R. S.: Late Quaternary environments in Ruby Valley, Nevada, Quat. Res., 37, 1–15, https://doi.org/10.1016/0033-5894(92)90002-Z, 1992.
- 1452 Thompson, R. S., Anderson, K. H., and Bartlein, P. J.: Atlas of Relations Between Climatic Parameters and Distributions of Important Trees and Shrubs in North America–Introduction and Conifers, U.S.
- 1454 Department of the Interior, U.S. Geological Survey, 1999.





- Thuiller, W., Lafourcade, B., Engler, R., and Araújo, M. B.: BIOMOD A platform for ensemble
- 1456 forecasting of species distributions, Ecography, 32, 369–373, 2009.
 - Trachsel, M., Dawson, A., Paciorek, C. J., Williams, J. W., McLachlan, J. S., Cogbill, C. V., Foster, D.
- R., Goring, S. J., Jackson, S. T., Oswald, W. W., and others: Comparison of settlement-era vegetation reconstructions for STEPPS and REVEALS pollen-vegetation models in the northeastern United States,
- 1460 Quat. Res., 95, 23–42, 2020.
 - Trondman, A.-K., Gaillard, M.-J., Mazier, F., Sugita, S., Fyfe, R., Nielsen, A. B., Twiddle, C., Barratt, P.,
- Birks, H. J. B., Bjune, A. E., and others: Pollen-based quantitative reconstructions of Holocene regional vegetation cover (plant-functional types and land-cover types) in Europe suitable for climate modelling,
- 1464 Glob. Change Biol., 21, 676–697, 2015.
- Trondman, A.-K., Gaillard, M.-J., Sugita, S., Björkman, L., Greisman, A., Hultberg, T., Lagerås, P.,
- Lindbladh, M., and Mazier, F.: Are pollen records from small sites appropriate for REVEALS model-based quantitative reconstructions of past regional vegetation? An empirical test in southern Sweden,
- 1468 Veg. Hist. Archaeobotany, 25, 131–151, 2016.
- Umbanhowar, Jr., C. E., Camill, P., Geiss, C. E., and Teed, R.: Asymmetric vegetation responses to mid-
- 1470 Holocene aridity at the prairie-forest ecotone in south-central Minnesota, Quat. Res., 66, 53–66, 2006.
 - United States Geological Survey: National Hydrography Dataset (NHD Model v2.3.1), 2022.
- van Vuuren, D. P., Stehfest, E., Gernaat, D. E. H. J., Doelman, J. C., van den Berg, M., Harmsen, M., de Boer, H. S., Bouwman, L. F., Daioglou, V., Edelenbosch, O. Y., Girod, B., Kram, T., Lassaletta, L.,
- Lucas, P. L., van Meijl, H., Müller, C., van Ruijven, B. J., van der Sluis, S., and Tabeau, A.: Energy, land-use and greenhouse gas emissions trajectories under a green growth paradigm, Glob. Environ.
- 1476 Change, 42, 237–250, https://doi.org/10.1016/j.gloenvcha.2016.05.008, 2017.
- Walsh, M. K., Whitlock, C., and Bartlein, P. J.: A 14,300-year-long record of fire-vegetation-climate linkages at Battle Ground Lake, southwestern Washington, Quat. Res., 70, 251–264, https://doi.org/10.1016/j.yqres.2008.05.002, 2008.
- Walsh, M. K., Pearl, C. A., Whitlock, C., Bartlein, P. J., and Worona, M. A.: An 11 000-year-long record of fire and vegetation history at Beaver Lake, Oregon, central Willamette Valley, Quat. Sci. Rev., 29,
- 1482 1093–1106, https://doi.org/10.1016/j.quascirev.2010.02.011, 2010.
- Walsh, M. K., Marlon, J. R., Goring, S. J., Brown, K. J., and Gavin, D. G.: A regional perspective on Holocene fire-climate-human interactions in the Pacific Northwest of North America, Ann. Assoc. Am. Geogr., 105, 1135–1157, 2015.
- Whitlock, C.: Vegetational and climatic history of the Pacific Northwest during the last 20,000 years: Implications for understanding present-day biodiversity, Northwest Environ. J., 8, 5–28, 1992.
- Whitlock, C., Colombaroli, D., Conedera, M., and Tinner, W.: Land-use history as a guide for forest conservation and management, Conserv. Biol., 32, 84–97, https://doi.org/10.1111/cobi.12960, 2018.
- Whitmore, J., Gajewski, K., Sawada, M., Williams, J., Shuman, B., Bartlein, P., Minckley, T., Viau, A., Webb Iii, T., Shafer, S., and others: Modern pollen data from North America and Greenland for multi-
- scale paleoenvironmental applications, Quat. Sci. Rev., 24, 1828–1848, 2005.





- Wieczorek, M. and Herzschuh, U.: Compilation of relative pollen productivity (RPP) estimates and 1494 taxonomically harmonised RPP datasets for single continents and Northern Hemisphere extratropics, Earth Syst. Sci. Data, 12, 3515-3528, 2020.
- 1496 Williams, J. W. and Jackson, S. T.: Novel climates, no-analog communities, and ecological surprises, Front. Ecol. Environ., 5, 475–482, https://doi.org/10.1890/070037, 2007.
- 1498 Williams, J. W., Shuman, B. N., and Webb, I., T.: Dissimilarity analyses of late-Quaternary vegetation and climate in eastern North America, Ecology, 82, 3346-3362, 2001.
- 1500 Williams, J. W., Shuman, B. N., Webb, T., III, Bartlein, P. J., and Luduc, P. L.: Late-Quaternary vegetation dynamics in North America: scaling from taxa to biomes, Ecol. Monogr., 74, 309–334, 2004.
- 1502 Williams, J. W., Shuman, B., and Bartlein, P. J.: Rapid responses of the Midwestern prairie-forest ecotone to early Holocene aridity, Glob. Planet. Change, 66, 195-207, 2009a.
- 1504 Williams, J. W., Shuman, B., and Bartlein, P. J.: Rapid responses of the prairie-forest ecotone to early Holocene aridity in mid-continental North America, Glob. Planet. Change, 66, 195-207,
- 1506 https://doi.org/10.1016/j.gloplacha.2008.10.012, 2009b.
- Williams, J. W., Tarasov, P. A., Brewer, S., and Notaro, M.: Late-Quaternary variations in tree cover at 1508 the northern forest-tundra ecotone, J. Geophys. Res. - Biogeosciences, 116, G01017, doi: 10.1029/2010JG001458, 2011.
- 1510 Williams, J. W., Grimm, E. G., Blois, J., Charles, D. F., Davis, E., Goring, S. J., Graham, R., Smith, A. J., Anderson, M., Arroyo-Cabrales, J., Ashworth, A. C., Betancourt, J. L., Bills, B. W., Booth, R. K.,
- 1512 Buckland, P., Curry, B., Giesecke, T., Hausmann, S., Jackson, S. T., Latorre, C., Nichols, J., Purdum, T., Roth, R. E., Stryker, M., and Takahara, H.: The Neotoma Paleoecology Database: A multi-proxy,
- 1514 international community-curated data resource, Quat. Res., 89, 156-177, https://doi.org/10.1017/qua.2017.105, 2018.
- 1516 Worona, M. A. and Whitlock, C.: Late Quaternary vegetation and climate history near Little Lake, central Coast Range, Oregon, Geol. Soc. Am. Bull., 107, 867–876, 1995.
- 1518 Zapolska, A., Serge, M. A., Mazier, F., Quiquet, A., Renssen, H., Vrac, M., Fyfe, R., and Roche, D. M.: More than agriculture: Analysing time-cumulative human impact on European land-cover of second half
- 1520 of the Holocene, Quat. Sci. Rev., 314, 108227, https://doi.org/10.1016/j.quascirev.2023.108227, 2023.

1522